12-2021

Classical Venturi Meter Performance Downstream of the Through Leg of a Tee Junction

Matthew P. Day
Utah State University

CLASSICAL VENTURI METER PERFORMANCE DOWNSTREAM OF THE THROUGH LEG OF A TEE JUNCTION

by

Matthew P. Day

A thesis submitted in partial fulfillment
of the requirements for the degree

of

MASTER OF SCIENCE

in

Civil and Environmental Engineering

Approved:

Michael C. Johnson, Ph.D., P.E. Major Professor	Zac Sharp, Ph.D., P.E. Committee Member
Austin Ball, M.S., P.E. Committee Member	D. Richard Cutler, Ph.D. Interim Vice Provost of Graduate Studies

UTAH STATE UNIVERSITY
Logan, Utah

2021

ABTRACT

Classical Venturi Meter Performance Downstream of the Through Leg of a Tee Junction

by

Matthew P. Day, Master of Science

Utah State University, 2021

Major Professor: Dr. Michael C. Johnson
Department: Civil and Environmental Engineering

The purpose of this research was to analyze the measurement accuracy of a Classical Venturi meter installed at various distances downstream on the through leg of a tee junction in a pipeline. Inaccurate readings from the Classical Venturi meter may cause revenue loss for companies or organizations involved in extraction, transportation, production, or purchasing of fluid resources and products.

One source of inaccurate flowmeter performance is improper meter installation according to published industry standards. These standards, however, cannot always be followed due to insufficient space or limited economic resources for meter placement. In these circumstances it is critical to understand how upstream flow disturbances, such as a tee junction, will affect the accuracy of a Classical Venturi meter.

This research compared the discharge coefficients of a Classical Venturi meter from a straight-line calibration to the discharge coefficients of the meter installed on the through leg of a bifurcating tee junction using numerical methods. The ratio of the two discharge coefficients is then used as a correction factor. The numerical models were calibrated and verified with physical data collected from a 6-inch Universal Venturi Tube.

Results show that a Classical Venturi meter is most accurate in this installation when more than 40% of the flow entering the tee junction is directed through the straight leg to the meter. As a larger portion of the water is drawn through the branch of the tee junction, the accuracy of the Classical Venturi meter decreases. Although physical laboratory calibrations remain the most effective way to ensure best metering capabilities, correction factors may be used to account for deviations due to such installation if laboratory testing is not possible.

(75 pages)

PUBLIC ABSTRACT

Classical Venturi Meter Performance Downstream of the Through Leg of a Tee Junction

Matthew P. Day

The purpose of this research was to analyze the accuracy of a Classical Venturi meter installed downstream of the through leg of a tee junction. A flowmeter that functions inaccurately due to improper installation may cause revenue loss for any company or organization involved in extraction, transportation, production, or purchasing of fluid resources and products. This research used physical data coupled with data produced by numerical models to determine how to correct the Classical Venturi meter's inaccuracies created by this particular installation.

Results show the capability of measuring the flow rate accurately was greatly affected when most of the flow was directed through the branch of the tee junction. As a greater ratio of water is directed through the meter, the accuracy increases. While physical laboratory calibrations remain the most effective way to ensure best metering accuracy, correction factors may be used to account for such installations if laboratory testing is not possible.

ACKNOWLEDGMENTS

I would like to thank Dr. Michael Johnson for the opportunity to spend over 3 years working at the Utah Water Research Laboratory (UWRL) while completing my undergraduate and graduate degrees. In my time at the UWRL, Dr. Johnson has mentored, guided, and taught me many valuable lessons to be applied academically, professionally, and personally. I appreciate the many hours of help collecting and analyzing data along with the professional advice and editing for this thesis.

I would also like to thank my committee members Dr. Sharp and Austin Ball for their time and support. Dr. Sharp played a critical role in helping me with computational fluid mechanics (CFD).

Gratitude goes out to my fellow UWRL researchers Taylor Stauffer, Hayden Coombs, Elliot Naulu, Ben Sandberg, and Riley Manwaring for their humor and stories to weather the hardships of time consuming computer simulations.

Most importantly I want to thank my wife, Kara, for the love, support and patience she has displayed during this endeavor. I owe all of this research and my whole life to you. I love you sweetheart.

Matthew P. Day

CONTENTS

Page

LIST OF FIGURES

Figure Page

Figure Page

LIST OF EQUATIONS

NOTATION

Definition

Beta – Ratio of throat diameter to inlet diameter of a flowmeter

CFD – Computation Fluid Dynamics

GCI – Grid Convergence Index

RANS – Reynolds Average-Navier Stokes turbulence model

UVT – Universal Venturi Tube

UWRL – Utah Water Research Laboratory

0D – The meter is installed zero diameters downstream of the tee junction on the through leg

5D – The meter is installed five diameters downstream of the tee junction on the through leg

CHAPTER I

INTRODUCTION

Purpose

The ability to accurately measure flow rate in pressurized pipelines is a critical aspect of many companies and organizations that extract, transport, or produce fluid resources such as crude oil, or products like drinking water or gasoline. Miscalculations in flow rate at any point throughout these processes may reduce overall revenue, result in over billing, and jeopardize product quality. Along with analyzing current operating conditions, accurate flow rate measurements also help guide future planning and construction. Flow rate data collected over many years is an indicator to determine if existing infrastructure has adequate capacity to meet projected demands or if the infrastructure needs to be improved or replaced.

There are many different types and styles of flowmeters, each unique in form, mechanisms, accuracy, and cost to meet varying project constraints. Pereira provides a list of many types of meters and how they function, some of which include: differential pressure producing meters, turbine meters, positive displacement meters, and ultrasonic meters (Pereira 2009).

Classical Venturi meters are simple, reliable, cost effective and commonly used throughout the industry. These meters are highly accurate when properly installed following established standards, created by the American Society of Mechanical Engineers (ASME), the International Organization for Standardization (ISO), and even certain meter manufacturers, that require a number of nominal lengths of straight pipe upstream and downstream of the meter (ASME 2007; ISO 2003). When these standards are not fulfilled and a meter is installed too close to upstream flow disturbances, like

elbows and tee junctions, flow rate accuracy may be compromised. To avoid decreased accuracy in these types of installations, the meter must be calibrated in a water research facility using the same pipe configuration and flow conditions. Laboratory calibrations require additional costs and time but remain the best alternative for assessing a flowmeter's performance.

There is some research available covering how metering capabilities for Classical Venturi meters, Halmi Venturi tubes, Wedge meters, Venturi Cone meters, HBX-1 meters, electromagnetic flowmeters, and ultrasonic meters are directly influenced by certain upstream flow disturbances such as pipe offsets and elbows. However, there is little research done that analyzes metering capabilities of a Classical Venturi meter downstream of a tee junction on the through leg.

The purpose of this research is to use computation fluid dynamics (CFD) to produce a cost effective alternate approach to mathematically improve a flowmeter's capabilities when industry standards of meter installation cannot be met due to space constraints or limited economic resources which prevent a laboratory or adequate field calibration.

The Utah Water Research Laboratory (UWRL) at Utah State University provided the resources needed to perform this research including instrumentation, pipes, meters, valves, computers, and software.

Objectives

The main objective of this research is to investigate the relationship between a differential pressure producing flowmeter's change in performance from a straight-line calibration to the calibration performed downstream of a tee junction installed on the through leg and the ratio of the meter's Reynold's number to the Reynold's number entering the tee junction. Collecting all of the data for this research in a laboratory setting was not possible because of time, space, cost and scheduling constraints. CFD methods were used to produce the data that were not obtainable in the laboratory. The use of CFD to identify trends in performance and its power as a predictive tool makes it a valuable resource in practice, as it is not feasible to physically model every possible permutation of pipe associate with flowmeter installation.

CFD is becoming a powerful engineering tool as numerical methods and computing technology have advanced. Although CFD has many applications and can be used to model setups difficult to achieve in the lab, it is important to understand how to get reliable results and reasonably interpret the data collected. For this reason, this research has a supporting objective to produce reliable CFD data by verifying and validating the CFD models used with limited physical data collected in the laboratory. These same CFD models are then applied to the rest of the simulations to collect the remaining data needed.

Scope of Work

With the wide variety of differential pressure producing flowmeters available and the numerous types of flow disturbances, an exhaustive study on this topic would surpass the available time for this research.

The scope of work for physical data is limited to analyzing a 6-inch Universal Venturi Tube (UVT) installed downstream on the through leg of a round cornered tee junction as seen in Figure 1. CFD analysis was then completed on the same 6-inch UVT and rounded corner tee junction to verify and validate the CFD models with the physical data. The same meter was then examined downstream of a sharp corner tee junction to compare the differences. In this same installation two 6-inch Classical Venturi meters, one with a beta value of 0.5 and the other having a beta value of 0.7, were tested.

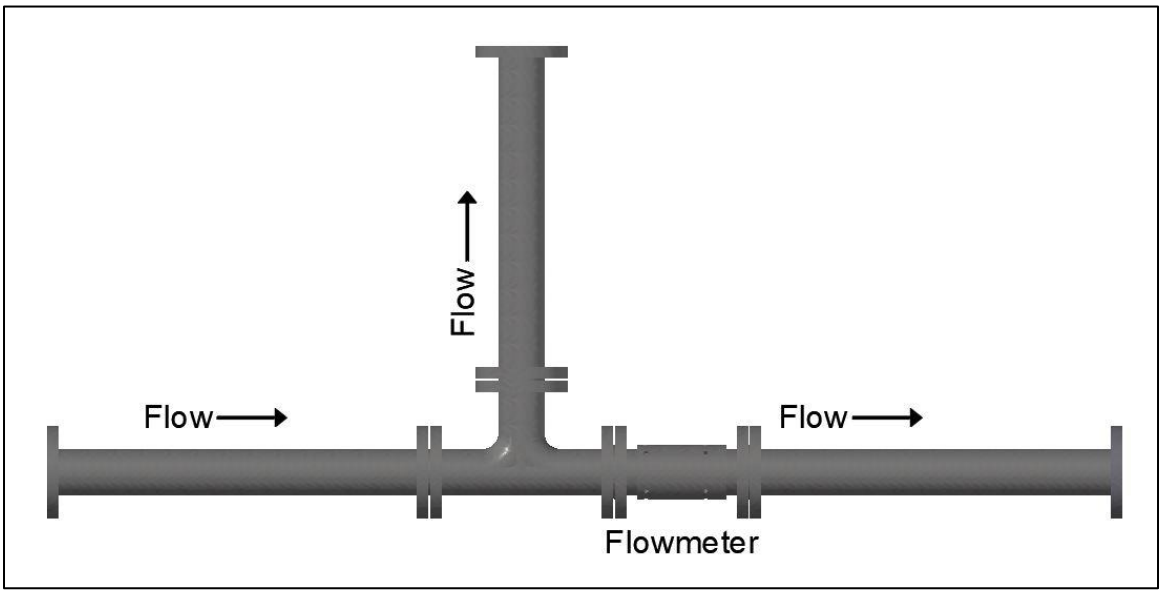

Figure 1. Classical venturi meter installed 0D of the through leg of a rounded corner bifurcating tee junction.

The remaining CFD work was narrowed down to investigate two 24-in. Classical Venturi meters, one with a beta value of 0.7 and the other with a beta value of 0.5. These meters were examined downstream of a sharp corner bifurcating tee junction on the through leg.

This scope of work allowed for accurate analyzation of the affects between rounded and sharp corner tee junctions, different flow rates and flow splits, changes in flowmeter size, the effects of a Classical Venturi meter and a UVT, and varying beta values for both meter types on metering accuracy. Appendix A provides a comprehensive list of installation setups, flow rates, and flow split ratios completed for this research.

CHAPTER II

LITERATURE REVIEW

Differential Pressure Meters

Differential pressure producing flowmeters are widely used around the world, especially the Classical Venturi meter. With the extent this product is used, the American Society of Mechanical Engineers (ASME 2005, ASME 2007) and International Organization for Standardization (ISO 2003) developed standards of installation and use. These standards outline that the required length of upstream pipe from a Classical Venturi meter is dependent on the meter's beta ratio. When these standards cannot be met and a meter must be installed closer to an upstream disturbance than prescribed by code, the meter performance may be compromised. The following section provides a summary of research relating to flowmeter performance installed downstream of flow disturbances.

Differential Pressure Meters with Upstream Disturbances

S.N. Singh et al. examined the performance of a V-cone meter installed at various downstream distances from a gate valve at opening conditions (Singh 2005). He concluded that the discharge coefficient of the meter is unaffected when the gate valve is installed at or more than 10 diameters upstream.

Bradford et al. researched the effects that a single elbow has on the accuracy of a Classical Venturi meter (Bradford 2006). Bradford's studies proved that meter accuracy in adverse installation conditions is largely dependent on the beta ratio of the meter. In addition, Bradford demonstrated that Classical Venturi flowmeters perform well when installed in conditions contrary to those suggest by ASME and ISO.

Radle investigated the performance of a Wedge flowmeter installed with different orientations at varying distances downstream from a double elbow out of plane (DEOP) disturbance. Radle found that the Wedge meter performance is not only controlled by distance of upstream pipe but also the orientation of the wedge. The results showed that the effect of the DEOP is reduced when the wedge is installed in plane with the second elbow (Radle 2016).

Day et al. supplemented the information in Radle's research by further examining the effects that the DEOP has on other meters such as a Halmi Venturi tube, Venturi Cone meter, Classical Venturi meter, and a HBX-1 meter. Day showed that the DEOP disturbance effects each meter in a unique manner and that some of those meters perform well in this installation (Day 2019).

Stauffer viewed this topic differently. Instead of looking at how disturbances directly effect a meter, Stauffer et al. investigated the possibility of mitigating errors caused by upstream disturbances by using multiple tap sets on a Classical Venturi meter instead of the industry standard of a single tap set. By doing so, Stauffer decreased the uncertainty and inconsistency of using one tap set by half when using the average of multiple tap sets (Stauffer 2019).

Sandberg conducted a study examining the effects that a bifurcating tee junction has on a 24-inch Classical Venturi meter installed on the branch leg. This research proved CFD is an effective tool to model flow and that creating contour plots of correction factors for overall flows against flow split ratios mathematically improves the meter's accuracy in those installations (Sandberg 2019).

Further research is needed to evaluate the effects that a bifurcating tee junction has on a Classical Venturi meter installed downstream of the through leg. The procedures and tools used in Sandberg's research will be used for this research due to the conditional similarities.

CHAPTER III

EXPERIMENTAL METHODS

Overview

The purpose of the experimental methods chapter is to make this research reproducible by providing procedural details for physical laboratory testing, numerical modeling, and graphical representations of results. The details provided in laboratory methods include descriptions of installation setups, a list of test instrumentation and an explanation of their purpose, a step by step procedure of how data points were collected, and pertinent equations. The numerical modeling methods describes the software package used to perform CFD for this research, outlines the setup for simulations, and explains how results are collected and verified. Lastly, the procedure for creating correction factors for the discharge coefficient using contour plots is provided in the final section of this chapter.

There are several common reference points for both the laboratory methods and numerical modeling methods presented here rather than in their respective sections.

For the remainder of this paper it important to know that straight-line installation means that there is more upstream pipe from the Venturi than required by ASME and ISO standards. Noteworthy is that these standards apply to the Classical Venturi meter design and do not apply to the short-form Venturi designs which include the Universal Venturi Tube (UVT) and Halmi Venturi Tube (HVT). It is also assumed that the reference of Venturi means Classical Venturi meter and when a reference is made to the Venturi being installed downstream of the tee junction, it is assumed to be installed downstream of the through leg. When this research mentions how far downstream the

Venturi is installed from the tee junction it will be called out with a number followed by the capital letter “D” to show how many pipe diameters separate the Venturi from the tee junction. For example, 2D means the Venturi is installed 2 nominal pipe diameters downstream from the tee junction.

For both the laboratory testing and numerical modeling, the static pressure readings at both the inlet, where high pressures occur, and in the throat, where there is low pressure, through what is called a tap. A pair of taps, one from the inlet and one from the throat on the same plane and side of the meter, is referred to as a “tap set”. Consistency in tap set location through both the laboratory testing and numerical modeling is critical to this research. Figure 2 demonstrates the locations of the 4 different tap sets used for this research. It is important to note that tap set 1 is always on the side of the tee junction. Tap set locations for the straight-line tests are similar omitting the tee junction.

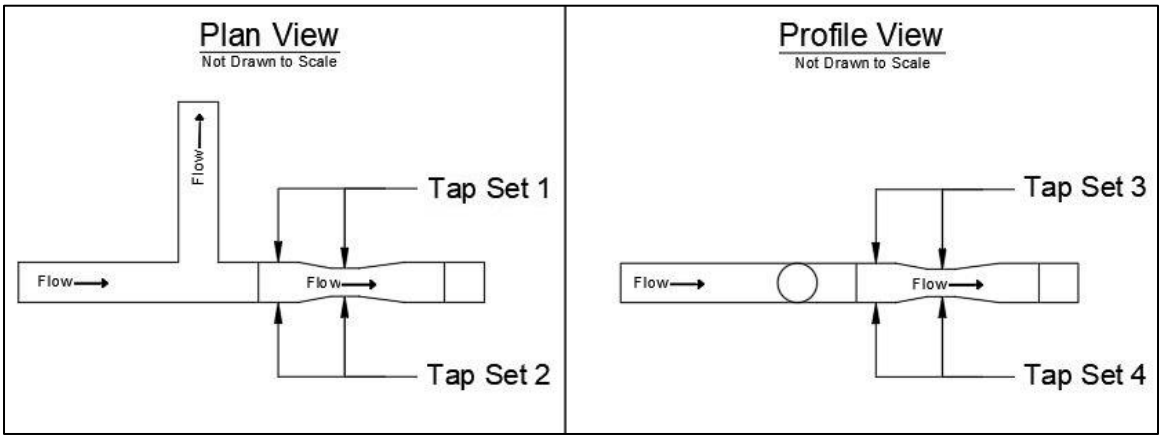

Figure 2. Determined locations for tap sets 1-4.

The data points collected during the laboratory testing and numerical modeling were differential pressure readings, total flow rates, and flow rates through the Venturi.

Methods for collecting these data points for each type of testing is described in detail in their respective sections.

When collecting data for an experiment there is always some degree of uncertainty. There are two main types of uncertainty that exist, systematic uncertainty and random uncertainty. Systematic uncertainty is a reoccurring error in measurements that causes a shift in the overall collection of data from the actual measurement. Random uncertainty happens when repeated measurements are taken but different values are produced causing variation in the data. Systematic and random uncertainty are prevalent in both the laboratory testing and numerical modeling. A discussion about how uncertainty is handled in each testing method is included in the following sections.

Laboratory Methods

The physical testing for this research was conducted at the UWRL. Over the years, the UWRL has accumulated a large inventory of pipes, connections, valves, meters, and much more. For the purposes of this study the UWRL had available a 6-inch UVT, a 6-inch rounded corner tee junction, and the required lengths of 6-inch steel pipe to complete the straight-line calibration and tee junction installations.

Before further discussing the methods used in the laboratory, it is important to explain the principals and equations that govern flow rate measurement with a Venturi. The design of the Venturi is such that the inlet portion of the meter is equal to or very close to the same diameter of the approaching upstream pipe. The inlet is followed by a converging section that reduces the diameter of the flow down to the throat of the meter. After the throat there is a diverging section that expands the diameter of the flow back to

the diameter of the pipe. Figure 3 shows the geometry of a 6-inch Venturi design according to ASME standards in ASME PTC 19.5-2004 with dimensions shown in inches or degrees, respectively.

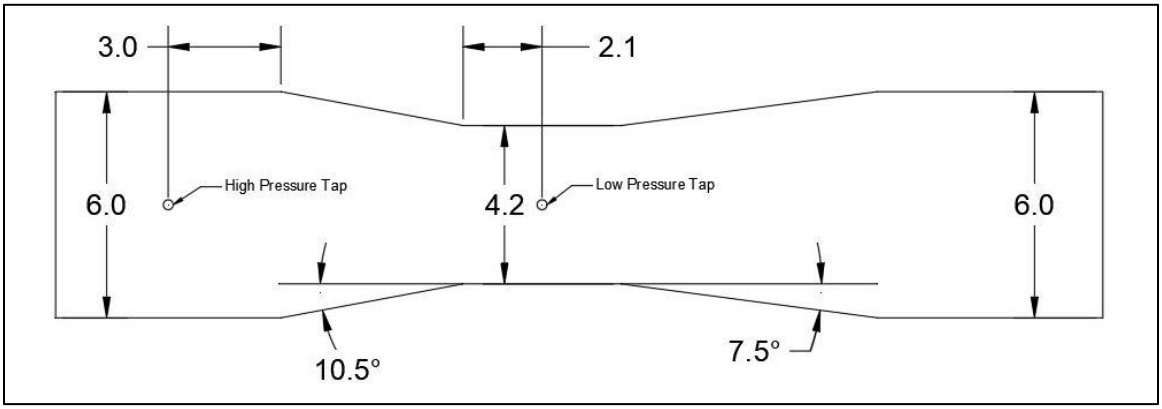

Figure 3. 6-inch 0.7 beta Classical Venturi meter design following ASME standards.

The following principals are based on the assumptions that the fluid is incompressible and that flow is fully developed at the meter inlet. The basic principal of conservation of mass provides an understanding to how the Venturi works. Equation 1 is the basic form of conservation of mass simply showing that what goes into a meter must come out. Since the flow rate must remain constant through the entire meter, as the cross sectional area decreases at the throat the velocity of the flow increases. According to Bernouli's principal when the velocity of a fluid increases, the static pressure decreases (Finnemore 2002). These two basic principles show how low pressures are created in the throat of the Classical Venturi meter.

$$Q = A_{inlet} * V_{inlet} = A_{throat} * V_{throat} \quad (1)$$

Equation 2 is derived from Bernoulli's Equation coupled with the conservation of mass and is used to calculate the theoretical flow rate of a Venturi.

$$Q_{calculated} = A_{throat} * \sqrt{\frac{2*g*\Delta P*\rho_{fluid}}{1-\beta^4}} \quad (2)$$

Where $Q_{calculated}$ is the calculated flow rate in pounds per second, A_{throat} is the area in feet squared of the throat, g is the dimensional conversion factor depending on units used, ΔP is the differential pressure reading between a high tap and a low tap, ρ_{fluid} is the density of the fluid flowing through the meter, and β is the ratio of the throat diameter to the inlet diameter.

Equation 2 is based on ideal assumptions that do not exist in the real world, meaning that the equation will not calculate the true flow rate through a Venturi unless it is adjusted by a discharge coefficient. A discharge coefficient is the ratio of the actual flow rate over the theoretical or calculated flow rate as demonstrated in equation 3.

$$C_d = \frac{Q_{actual}}{Q_{calculated}} \quad (3)$$

This means that the actual mass flow rate is calculated using equation (4)

$$Q_{actual} = C_d * A_{throat} * \sqrt{\frac{2*g*\Delta P*\rho_{fluid}}{1-\beta^4}} \quad (4)$$

When both sides of the equation are dividing by the density of the fluid, equation 5 is produced which calculates volumetric flow.

$$Q_{actual} = C_d * A_{throat} * \sqrt{\frac{2*g*\Delta P}{(1-\beta^4)*\rho_{fluid}}} \quad (5)$$

Laboratory calibrations of meters are critical in determining discharge coefficients and ultimately having a reliable meter. Accurately measuring the actual flow rate in the laboratory is one of the most important steps of the calibration. For this research 25,000 pound and 250,000 pound NIST traceable weigh tanks were used to measure actual flow rate. The National Institute of Standards and Technology (NIST) is a non-regulatory

agency of the United Stated Department of Commerce that ensures instrumentation accuracy. This research calculated actual flow rate using equation 6.

$$Q_{actual} = \frac{W_{collected}}{\rho_{fluid} * T_{test}} \quad (6)$$

Where Q_{actual} is the actual flow rate in cfs, $W_{collected}$ is the weight of the water collected during the test, $\rho_{fluid}$is the density of the fluid in the weight tank, and T_{test} is the time that the water was collected in the tank. The temperature of the water was taken to determine density of the fluid by interpolating values on a table provided in "Flow Measurement Engineering Handbook" (Miller 1996).

A diagram for the physical straight-line testing is shown in Figures 4 with an image of the actual straight-line setup in Figure 5. In Figure 4 the total flow enters from left to right, passing through the reference flowmeter. The flow is then redirected through a series of 90-degree elbow connections to redirect the flow from right to left. More than sufficient pipe lengths were installed downstream from the second elbow to meet AMSE installations standards for a Classical Venturi meter of this beta value although the meter tested was a UVT. Flow then passes through the UVT downstream to a control valve and eventually into one of the two NIST traceable weight tanks depending on the magnitude of the flow rate.

The second set of installations, where the meter is placed downstream of the tee junction is depicted by the rendering in Figure 6 and Figure 7 demonstrates what the physical setup for this test looked like in the laboratory.

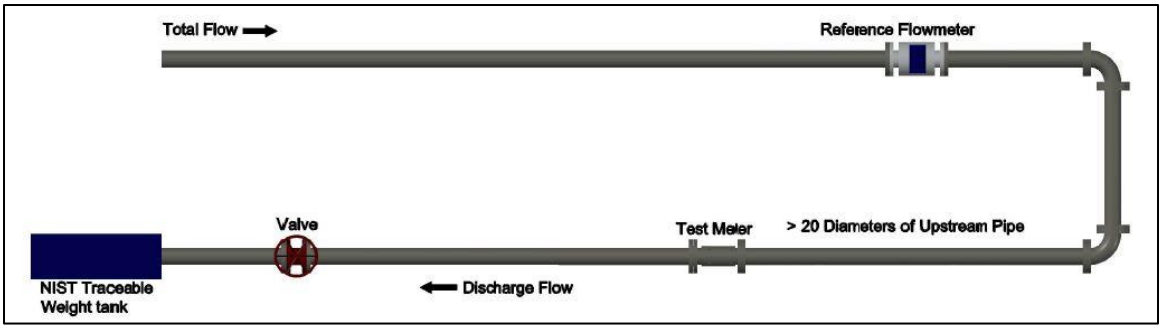

Figure 4. Laboratory setup for a straight-line calibration.

Figure 5. Laboratory straight-line calibration.

It is important to note that the reference flowmeter had been verified against the weight tank to accurately measure flow within ±0.25% for the flow rates used in this research. This is important because the next set of physical testing placed the UVT downstream of a tee junction, as seen in Figure 5, where some of the flow is wasted into a channel. In order to know the percentage of the total flow entering the UVT, an accurate measurement of the total flow rate is needed.

For this testing the reference flowmeter was wired to a multi-meter. The multi-meter reads a hertz output from the reference flowmeter to indicate the flow rate reading. Multi-meters were used because of the real-time averaging capabilities that they have. The differential pressure across the pressure taps of the UVT was measure using a differential pressure transmitter. The differential pressure transmitter was wired to a multi-meter so that the differential pressure of the UVT could be averaged in real-time as a voltage output from the transducer. Diagrams demonstrating the multi-meter connections to the reference flowmeter and the pressure transducer are provided in Appendix B.

The procedure for conducting a physical straight-line calibration for the UVT is listed below:

1) Set the desired flow rate with the control valve
2) Start averaging the multi-meter wired to the reference flowmeter
3) Simultaneously average the multi-meter wired to the pressure transducer
4) Let averaging values stabilize
5) Record the stabilized averaged values for flow rate and differential pressure
6) Record the temperature of the water from temperature probe

A similar setup was used for the physical tee junction testing of the UVT. Figure 6 presents a diagram of the general setup, however, the UVT was tested both at 0D, or directly bolted to the through leg of the tee junction, and also 5D downstream from the tee junction as seen in Figure 7 and Figure 8.

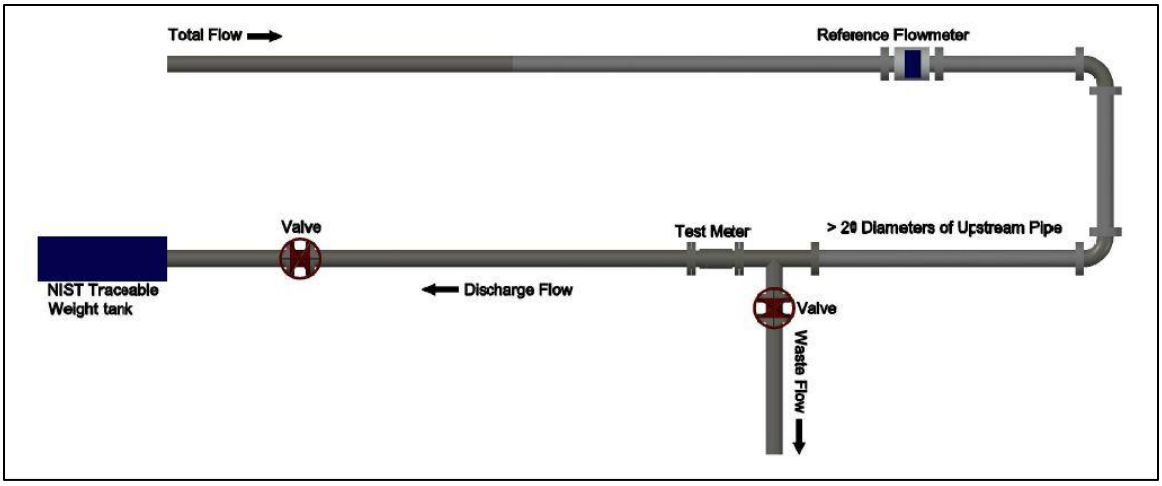

Figure 6. Laboratory setup for a 0D tee junction calibration.

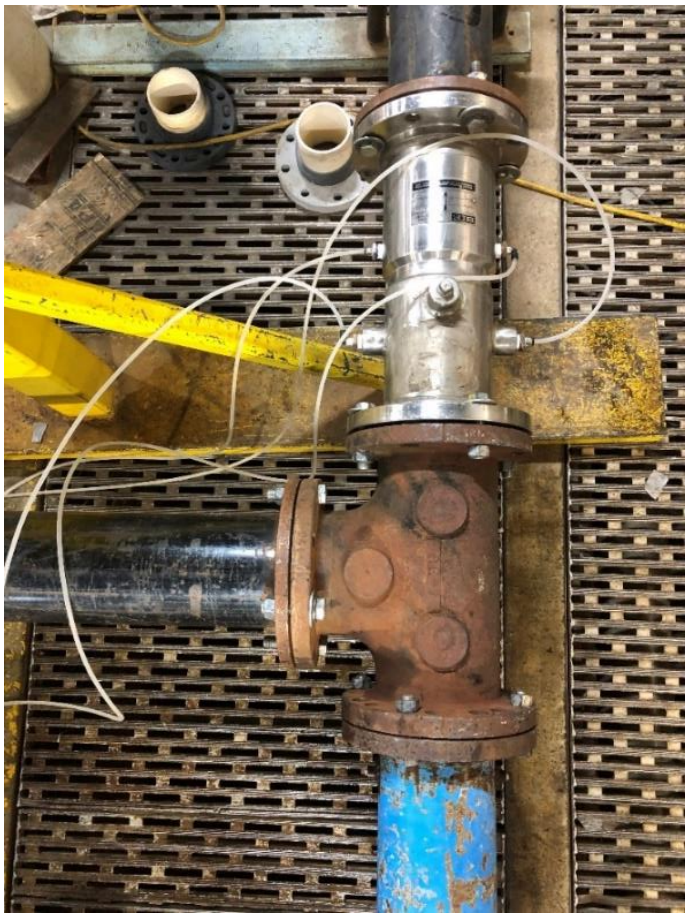

Figure 7. UVT with taps at positions 1 and 2 installed 0D on the through leg of a round cornered tee junction.

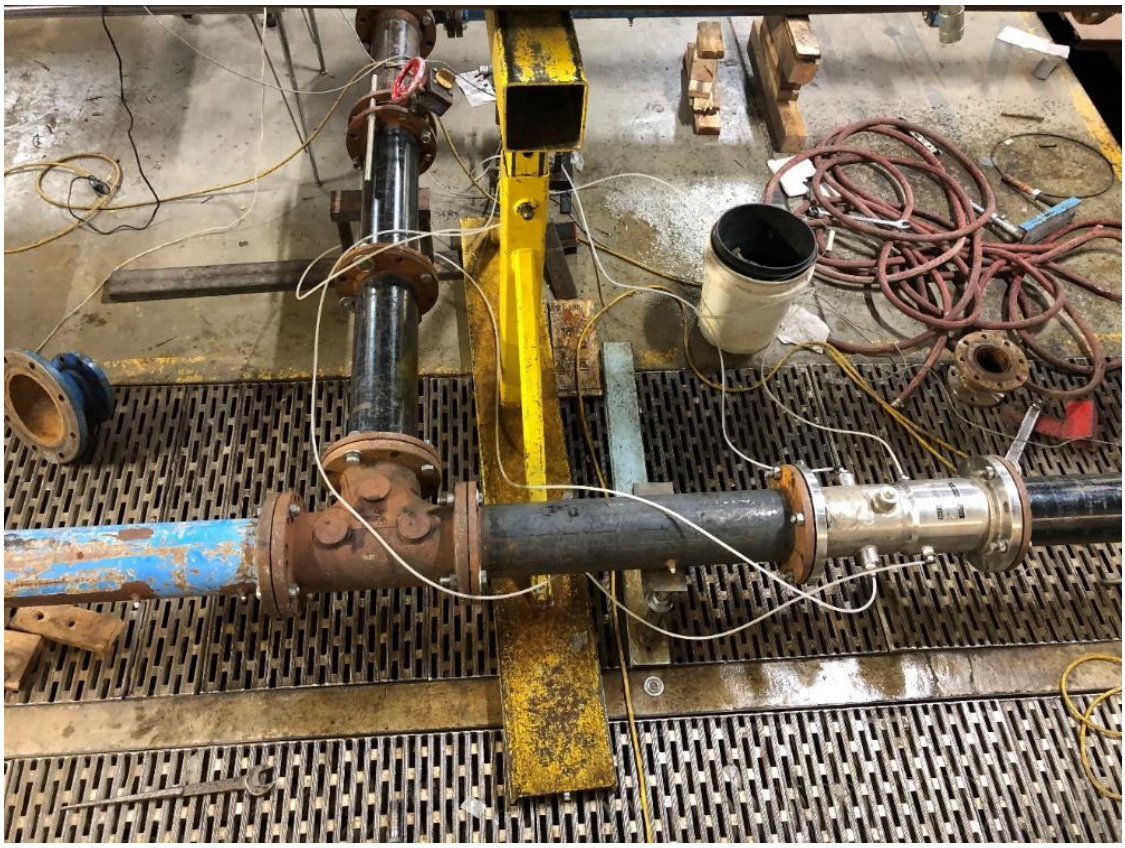

Figure 8. UVT with taps at positions 1 and 2 installed 5D on the through leg of a round cornered tee junction.

The procedure followed for conducting the tee junction calibrations for the UVT is listed below:

1) Use both control valves to set desired total flow rate based on reference flowmeter reading and desired flow through the UVT based on the UVT flow rate reading from the straight-line calibration
2) Start filling the weight tank while simultaneously
    a. Start the stop watch
    b. Note the beginning weight of the tank
    c. Average the multi-meter wired to the reference flowmeter.

d. Average the multi-meter wired to the pressure transducer.

e. Let the desired time for the test pass

3) Stop filling the tank while simultaneously

a. Stop the stop watch

b. Note final weight of tank and record the temperature of the water

4) Record the averaged values from the multi-meters

For these tests the author utilized two different weight tanks, one with the capacity to hold 25,000 pounds and the other with a capacity of 250,000 pounds. The smaller weigh tank requires the use of a stop-watch as mentioned in the above steps. The larger weight tank has a programmed control that starts and stops the flow over a specified time period. For all of the data collected with the 250,000 lb. weight tank, the author followed the same steps as listed above without the use of a stopwatch.

Understanding how to properly use the instrumentation to take measurements is a fundamental part of this research. In the laboratory there are five measurements taken for each data point. For each one of these measurements, there is a specific instrument or series of instruments used. Each instrument is described and the procedure followed for taking measurements outlined in the following paragraphs.

The first measurement to be taken is the total flow rate through the reference meter. Before the testing for this research began, the reference meter was calibrated in line with an accuracy of ±0.25%. The reference meter is wired to a multimeter, seen in Figure 9, where a voltage output is read and converted back to flow in gallons per minute by dividing the voltage by the quantity 4. The multimeter is used in this scenario for the averaging capabilities that it has. The flow from the reference meter is averaged over the

entire run using the multimeter, where once the run is complete, the flow is recorded as a voltage to the nearest whole number and then converted back into the flow rate. The accuracy of this method of measurement is a half a volt or 0.25 gallons per minute for each reading. This means that the actual flow rate could be ±0.25 gallons per minute which when referencing the lowest total flow rate measured in the lab is ±0.05%.

Figure 9. Multimeter used to average total flow and differential pressure.

The second measurement for this research is the differential pressure across the UVT. The differential pressure is measured using a pressure transmitter, as seen in Figure 10, wired to a multimeter for the averaging capabilities. The setup allows the user to measure the differential pressure in terms of voltage to three decimal places when the

voltage is 2 or higher and four decimal places when the voltage is between 1 and 2. These means that when the voltage is between 1 and 2 this method of measurement has an accuracy of ±0.0001 volts, which converts to ±0.07%, and ±0.001 volts when the output is greater than 2 representing an accuracy of ±0.08% in differential pressure reading of head in inches.

Figure 10. Pressure transmitters used to measure differential pressure.

The third measurement recorded is the temperature of the water in the pipeline. This measurement is taken using a temperature probe, shown in Figure 11, inserted into the pipeline where the temperature is read directly in degree Fahrenheit to one decimal place. The temperature is then used to calculate the density, in pounds per cubic foot, and kinematic viscosity, in squared feet per second, of the water. A ±0.1 degree Fahrenheit

change in temperature gives a density accuracy within ±0.0005% and an accuracy for the kinematic viscosity of ±0.16%

Figure 11. Temperature probe installed on the test pipeline.

The fourth measurement for this research is the weight of the water collected in the NIST traceable weight tanks during the run time. There are two different instruments used for this measurement based on the quantity of water being collected during the run. When less than 10,000 pounds of water is collected, the small weight tank, as seen in Figure 12, with a capacity of 25,000 pound is used. This tank has the ability to read weight to ±5 pounds which for the lowest amount of weight collected for this study is ±0.17%. For weights above 10,000 pounds, the large weight tank with a capacity of

250,000 pounds is used as depicted in Figure 13. The large weight tank reads the weight to ±20 pounds which for the lowest weight collected in this tank is ±0.21%.

Figure 12. 25,000 pound NIST traceable weight tank

Figure 13. 250,000 pound NIST traceable weight tank

The final measurement recorded is time, in seconds, of the duration of the run. When using the small weight tank, the time is measured using a certified traceable stopwatch, as shown in Figure 14, that reads the time to ±0.01 seconds. The shortest time used for a run is 200 seconds which gives the stop watch an accuracy of ±0.005%. When the large weight tank is used for collecting water, there is an automatic control set to a user defined time. This control has an accuracy of ±0.082% for runs that are 200 seconds long which was used for this research.

Figure 14. Certified traceable stopwatch.

To quantitatively determine the uncertainty combining all 5 physical measurements the author followed the guidelines in ASME PTC 19.1 2005 test uncertainty national standard. At a 95% confidence interval the maximum calculated uncertainty for the physical data in this research is 0.78% with an overall average uncertainty of 0.21%. The largest uncertainties were for cases in which the meter was installed at 0D with flow splits of 20%, where high flow turbulence existed within the meter.

Numerical Modeling Methods

CFD modeling is emerging as a cost-effective and time saving alternative to physical models as the complexity of engineering problems increase and the solutions rely more heavily on robust and accurate research data. This research in particular

requires data to be collected from setups with different flowmeter types and sizes, installation placements, and beta ratios. Collecting all of this data in the laboratory would be costly due to the need to acquire the physical components and require a large amount of time and manpower. CFD software, however, provides the author with the ability to collect nearly all of this data with no added costs and no extra manpower. The author used Star CCM+ version 13.06.012-R8, a CFD software package from Siemens, to run simulations for this research.

Developing a simulation with Star CCM+ is a complex process and requires substantial experience with the software. The general procedure for developing a simulation and extracting results will be outlined within this section. Any details not provided regarding specific software details are found in the user manual for Star CCM+ (Siemens, 2020). The general outline for creating a CFD simulation is:

1. Create geometry of the three-dimensional flow volume.
2. Produce a part from completed geometry and properly label part surfaces.
3. Define a region for each part surface and select the correct boundary conditions.
4. Select the mesh and physics models to be used in the simulation.
5. Create the volume mesh.
6. Make scenes and plots to monitor simulation conditions.
7. Run simulation until the solution has converged.
8. Analyze scenes and plots with engineering judgement to ensure the correct solution has been reached.
9. Record data.

The author chose to use the surface remesher, polyhedral mesher, and prism layer mesher for the meshing models. The physics models used for simulations were three dimensional, steady, liquid, constant density, segregated flow, turbulent, exact wall distance, gradients, k-epsilon turbulence, realizable k-epsilon two-layer, Reynold-averaged navier-stokes (RANS), and two-layer all y+ wall treatment. With these models selected, the simulation software will simultaneously solve the continuity equation, momentum equation in each direction, turbulent dissipation rate, and turbulent kinetic energy for each iteration.

Each time the simulation completes an iteration, it calculates and plots the maximum difference in the solution for each of the equations listed above from the previous iteration. This plot is known as the residuals. With each iteration, the simulation approaches the solution, meaning that the difference in answers between iterations, or the residuals, of each governing equation gets closer to zero. Each simulation was run until all the residuals were below 10^{-5}, which is well past the threshold where the change in solution from iteration to iteration affects the data. In addition to monitoring the residuals, the author closely checked other aspects of the model to ensure quality data was taken.

In turbulent flow a viscous sublayer develops near boundaries, like a pipe wall, where the magnitude of velocity approaches zero. To determine how well this viscous sublayer is modeled the wall y+ value, a dimensionless distance that describes the fineness of mesh at a given flow rate, is calculated according to equations 7 and 8 and should be below 5 and optimally close to the value of 1 (Salim 2009).

$$wall\ y^+ = \frac{y * u_t}{\nu} \tag{7}$$

$$u_t = \sqrt{\frac{\tau_w}{\rho}} \tag{8}$$

Where in equation 7, y is the distance from the cell centroid to the nearest wall, u_t is the shear velocity, and ν is the kinematic viscosity. Equation 8 is used to calculate the shear velocity with τ_w being the wall shear stress and ρ is the fluid density.

To analyze the conditions of the simulation as it ran, the author created scalar scenes to monitor velocity, pressure, and wall y+ values throughout the flow volume. These scenes were used to visually represent the solutions that the computer produced. With these visual scenes, the author checked each simulation to make sure that flow fully developed before enter the tee junction, that pressure decreased adequately from upstream to downstream, and that the wall y+ values were around 1.

Once the residuals drop below 10^{-5}, the mesh has been adjusted so that the wall y+ values are correct, and the velocity and pressure scenes look accurate the data point is collected. Pressure probes located where the pressure taps would be were used to extract differential pressure data from the meter. Sectional planes located at the tee junction inlet and at the meter were also used to get mass flow rates to calculate the flow split through the tee junction and the meter Reynolds number for each simulation.

Once a simulation has been developed properly, it is important to run a grid or mesh independence study to eliminate, if possible, or reduce any influence that varying mesh sizes have on the results. The procedure for running a grid independence study is outline by Celik (Celik et al. 2008). This procedure allows the user to calculate the overall uncertainty in the solution between simulations run with two different base sizes to determine if the solution is independent of the mesh cell's base size.

Following this procedure for the 6-inch simulations on each tap set the maximum uncertain with a base size of 0.35-inches was 0.87%. Another grid convergence study was conducted for the 24-inch simulations and concluded that the maximum uncertainty for any one of the four tap sets with a base size of 2-inches was 0.82%. For the purposes of this research these are acceptable bounds of uncertainty. Simulations could be conducted with a smaller base size to reduce the level of uncertainty, consequently reducing the base size drastically increase the time to run a simulation. For this reason these cell base sizes were selected for this research.

Graphical Representation of Results

Graphical representation of the CFD simulation results is a key component to proper analyzation and use of the results by readers. Contour plots of discharge coefficient ratios plotted against flow splits and meter Reynolds number were created using code created by Ben Sandberg and Taylor Vaughn. Ben Sandberg previously used this code to successfully create contour plots of discharge coefficient ratios for a Classical Venturi meter installed on the branch leg of a tee junction. Due to the similarities between Sandberg's and this research, those interested in further researching this topic or those using this research for professional matters will be benefitted by a consistent methodology for producing these contour plots. Specifics concerning this methodology are provided in Appendix C of Sandberg's thesis (Sandberg, 2019). All contour plots for this research are found in Appendix A. Note that the Meter Reynolds number does not converge to zero for the data collected.

CHAPTER IV

RESULTS AND DISCUSSION

CFD Verification and Validation

To verify CFD as a useful modeling tool for this research, it needs to be validated with the physical data collected. The first data to validate is the 6 inch straight-line calibration performed on the UVT. The laboratory results for this calibration show that Tap Set 1 and Tap Set 2 had average Cd values of 0.9818 and 0.9794 respectively over a Reynolds Number range of 80,000 to 660,000. Over the same Reynolds Number interval, the CFD results showed that Tap Set 1 and Tap Set 2 had average Cd values of 0.9676 and 0.9675 which are 1.44% and 1.21% lower than the physical data. Figure 8 is a plot of the physical and CFD data interpolated at similar Reynolds Numbers. The nature of the plot for Tap Set 1 using CFD is similar for Tap Set 2, Tap Set 3, and Tap Set 4 using CFD.

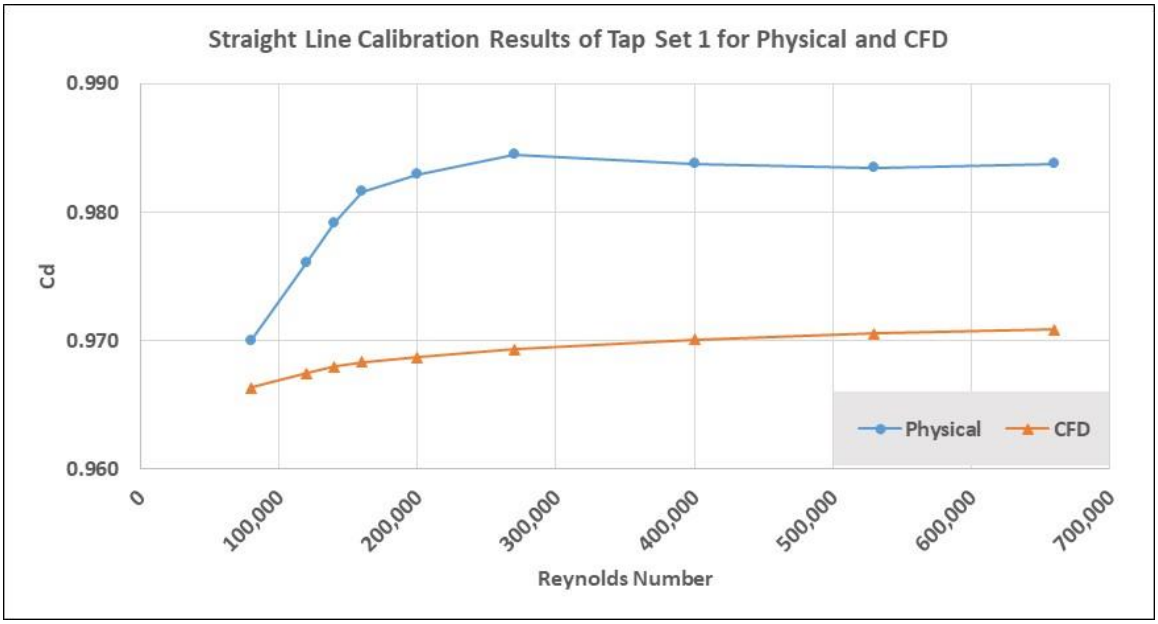

Figure 15. Plot of discharge coefficient, Cd, versus Reynolds number for the physical and CFD straight-line UVT calibration. These are typical values for all tap sets.

This research is not focused on the CFD results matching the physical data exactly, but rather that the CFD functions as an accurate tool to predict trends as variables are changed. Figure 9 demonstrates that the CFD results at a 0D installation over the entire range of flow splits follows a similar trend as the physical data. It is important to note that each point at each flow split is directly compared to the straight line discharge coefficient having the same Reynolds number at the meter and not to an averaged value. It is observed that the CFD data is shifted down consistently for Tap Sets 1, 2, and 3.

This shift could be a result of the limited modeling capabilities of the physical models used for the simulations. However, since the same physical models are used throughout the research, the same shift is introduced into every simulation. Since the analysis of the data is focused on how the $C_d$values change from the straight-line calibration to the specific tee junction installations, this shift is not important. It is

important to note that for all data collected Tap Set 3 is typical of Tap Set 4 due to symmetry, for this reason Tap Set 4 is not plotted.

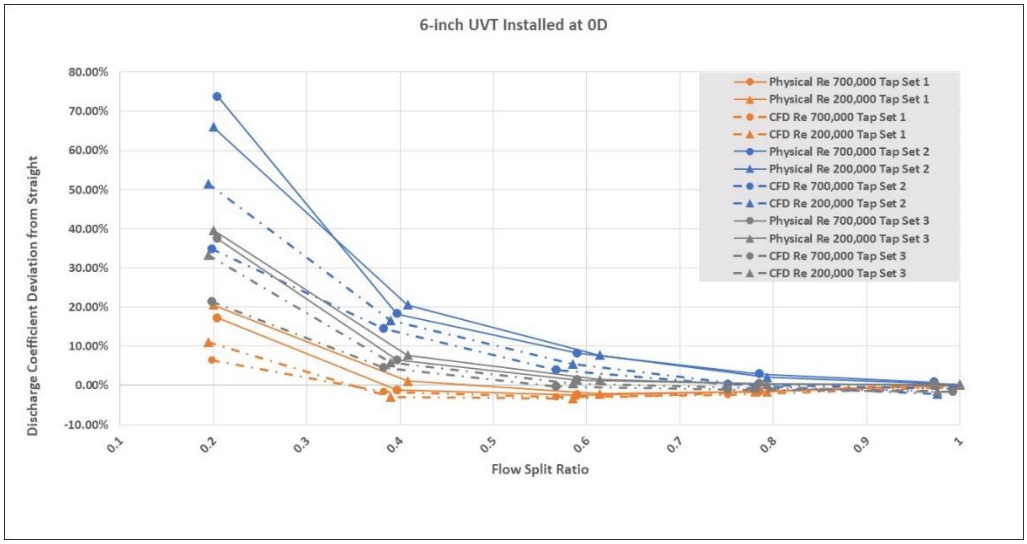

Figure 16. Plot of discharge coefficient deviation from straight versus flow split for the 6-inch UVT installed 0D from a round cornered tee junction.

Similarly, when the UVT meter is modeled at 5D downstream from the tee junction, represented by the data in Figure10, CFD again closely follows the trends developed by the physical data. For both Tap Set 1 and 2 at the 40% and 20% flow splits the CFD trends slightly different from the physical data, however, the scale on the independent axis is so narrow compared to Figure 9 above that this change is trend is negligible.

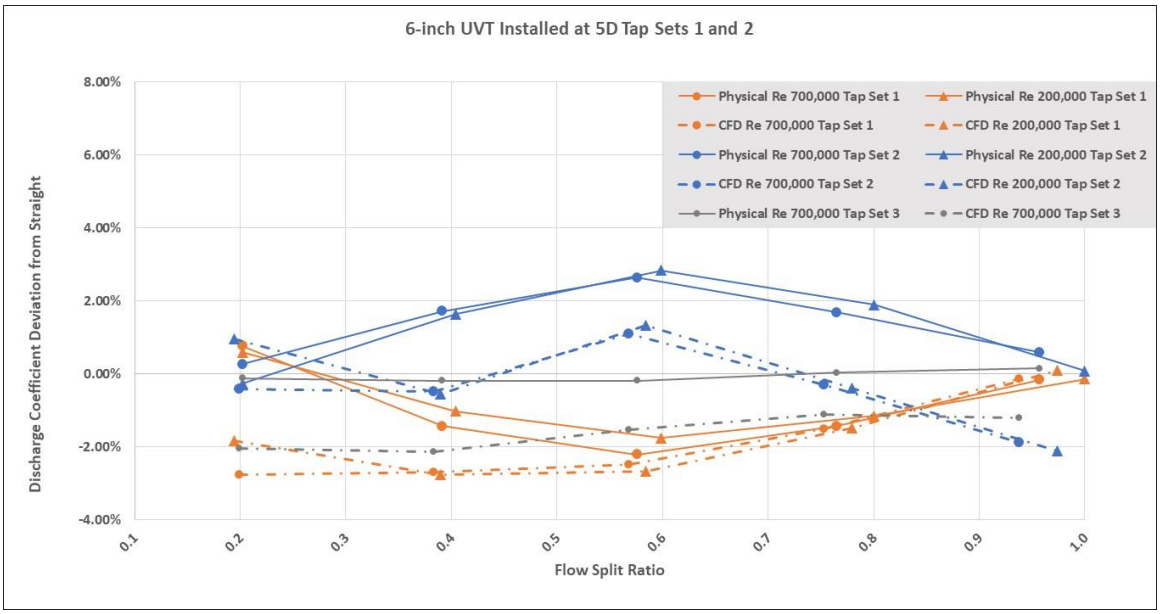

Figure 17. Plot of discharge coefficient deviation from straight versus flow split for the 6-inch UVT installed 5D from a round cornered tee junction.

The data presented in Figures 9 and 10 validates CFD's capability to accurately model both the discharge coefficient of a flowmeter in a straight-line calibration over a range of Reynolds numbers and the trend of the discharge coefficient deviation from straight over the entire range of flow splits at the specified distances downstream from the tee junction.

Figures 9 and 10 along with Figures B1 and B2, showing data for a 24-inch Classical Ventrui meter with a beta value of 0.7 installed at 0D and 5D respectively at four different main Reynolds Number, prove that the data for each tap set with varying setup configurations is tightly grouped together. These tight groupings prove that the discharge coefficient deviation from the straight-line calibration is not dependent on the total flow rate entering the system, but rather dependent on the actual flow split occurring in the tee junction.

Tee Junction Geometry

Now that CFD has been verified and validated as a viable tool to model these hydraulic setups, the effects of the proposed variables will be examined commencing with the geometry of the tee junction. The two tee junctions used for this analysis were a typical round cornered tee junction and a sharp cornered tee junction, for which dimensions are found in Appendix B.

The data presented in Figure 11 shows a comparison of the 6-inch UVT meter installed 0D from both a sharp and round cornered tee junction to the data collected on the 6-inch UVT meter in the lab. There is little variance in meter performance for Tap Set 1 between the round and sharp cornered tee junction installation apart from the 20% flow split where the sharp cornered tee junction installation follows the physical data more closely than the round cornered tee junction installation.

For Tap Sets 2 and 3 the data for the sharp cornered tee junction follows the physical data within ±1.5% for flow splits between 40% and 100%. Neither the sharp nor round cornered tee junction installations modeled the 20% flow split very well with a minimum variation of 12% from the physical data. Although the data does not match at the 20% flow split, it does follow a similar trend meaning that the modeling capabilities of physical models selected in Star CCM+ do not fully accommodate the turbulence in the flow under these conditions, but performs well enough for this analysis.

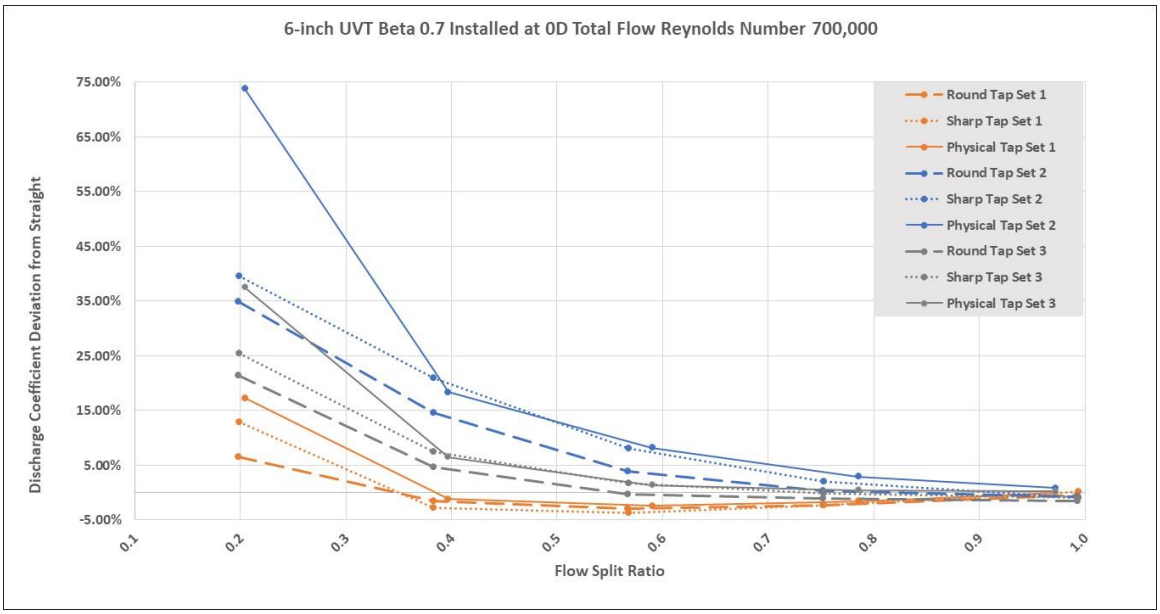

Figure 18. Plot of discharge coefficient deviation from straight versus flow split for the 6-inch UVT physical data and 6-inch UVT CFD models 0D from a round cornered and sharp cornered tee junctions.

Figure 12 presents the data for the same conditions as mentioned above with the UVT meter installed at 5D. It is clear that by 5 diameters downstream of the tee junction, both round and sharp cornered, metering accuracy improves drastically. All data points in Figure 12 fall within +2.8% and -4.8% deviation from the straight-line calibration. Under these conditions, Tap Set 1 is modeled more closely by the round cornered tee junction, the physical data for Tap Set 2 is modeled more accurately by the sharp cornered tee junction, and Tap Set 3 demonstrates that both the round and sharp cornered tee junction produce the same results falling 0.5% to 2.0% below the physical data over the range of flow splits.

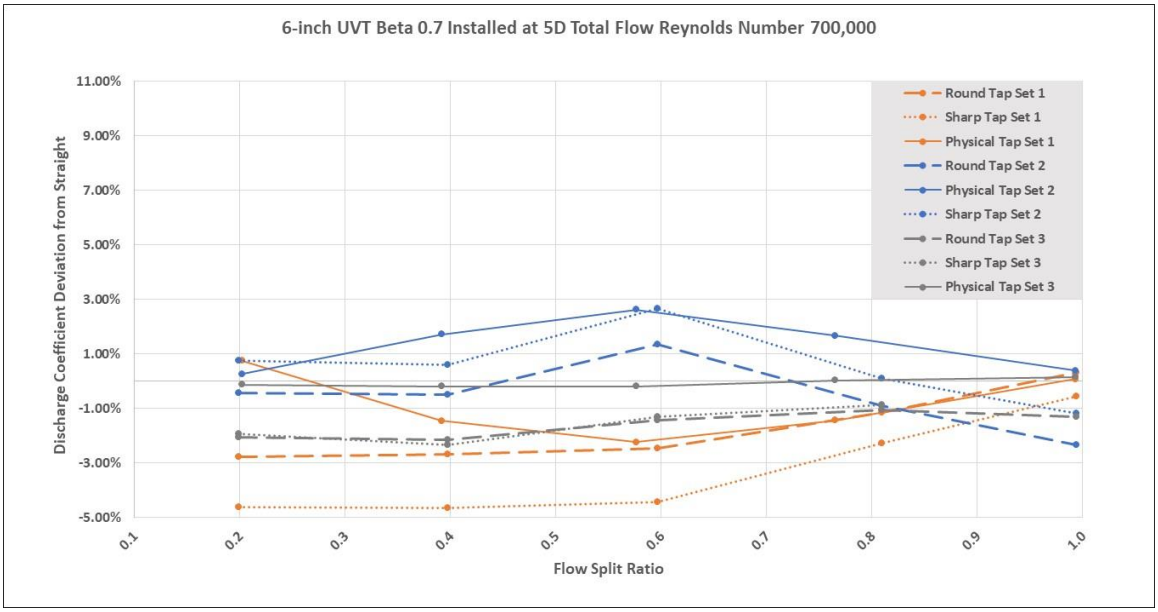

Figure 19. Plot of discharge coefficient deviation from straight versus flow split for the 6-inch UVT physical data and 6-inch UVT CFD models 5D from a round cornered and sharp cornered tee junctions.

Both the round and sharp cornered tee junctions accurately model the trends developed by the physical data. Although the change in tee junction geometry does cause a slight shift in the results, it does not change the overall trend. This analysis concludes that tee junction geometry contributes a minor role in the results and but is considered an independent variable for this research.

Pipe Size

Another variable to consider for this research is the size of pipe being used for the installation. For this analysis, a Classical Venturi meter with 0.7 beta value was modeled in both a 6-inch and a 24-inch line 5D from a sharp cornered tee junction. Figure 13 presents the data from these simulations.

Figure 13 shows that there is at most a 0.6% shift in deviation from the straight-line calibration between the 6-inch and 24-inch pipe sizes. Another observation to be made is that the trends developed by the larger pipe size tend to be smoother and less susceptible to variations in results from one flow split to the next. It is also important to note the scale on this graph and realize just how close these data points really are over the entire range of flow splits. This analysis concludes that the change in results due to varying pipes sizes is negligible for this research.

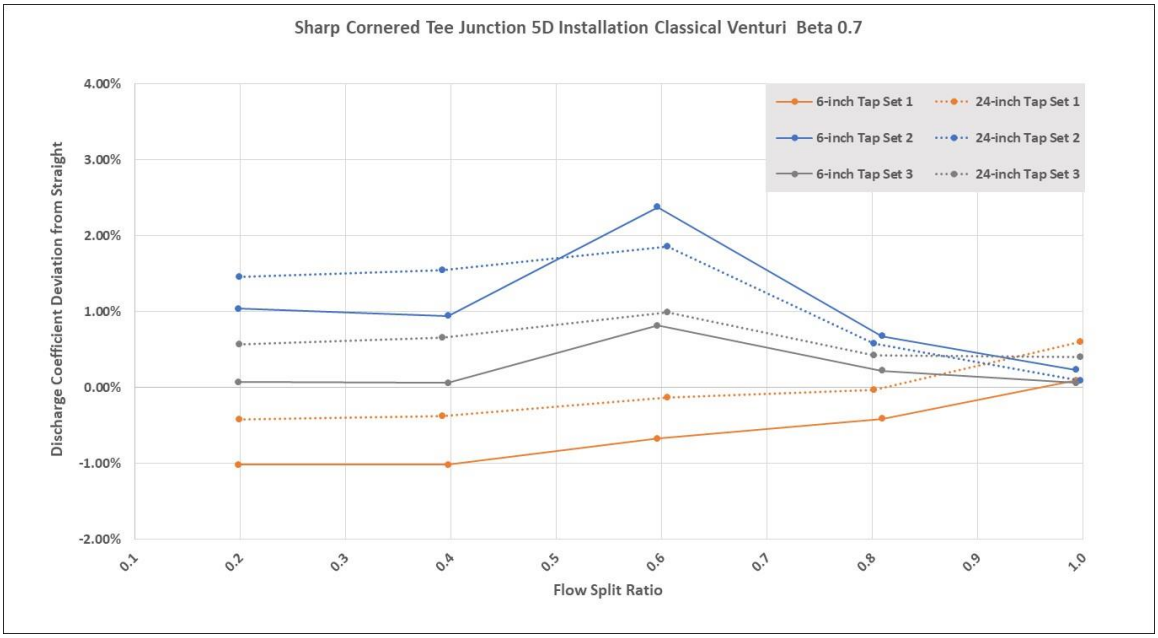

Figure 20. Plot of discharge coefficient deviation from straight versus flow split for a 6-inch and 24-inch Classical Venturi with 0.7 beta installed 5D from a sharp cornered tee junction.

Meter Type

Another variable to analyze for this research is how different meters perform under the same installation conditions. For this analysis a 6-inch UVT meter and a 6-inch

Classical Venturi meter, both with a beta value of 0.7, were simulated at 5D from a round cornered tee junction with a main inlet Reynolds Number of 700,000.

The results from these simulations is presented in Figure 14. The information in this graph shows that each type of meter has specific benefits and challenges. The 6-inch UVT meter has well developed trends for each tap set over the entire range of flow splits with one exception, Tap Set 2 at 60% flow split. However, the spread in deviation from the straight-line calibration between each tap set is 2.5-4% over most of the flow splits. This shows that which tap set you choose to use is critical to the overall metering capabilities.

The 6-inch Classical Venturi meter, on the other hand, has a spread of at most 1.5% between data points at the same flow split, with most points falling within 0.5% of one another. The challenge that the Classical Venturi meter faces is the unpredictability in the trend line at the 60% flow split. If the trend were stable, then the points at a flow split of 60% would be around -2.6% deviation from straight, however, these points land up between -0.2% and +1.5% deviation from straight.

This analysis shows that each meter type has benefits and challenges that the user needs to understand and approach correctly for their unique metering application. Meter type is a very important variable in this research having a substantial impact on the overall trends of the data.

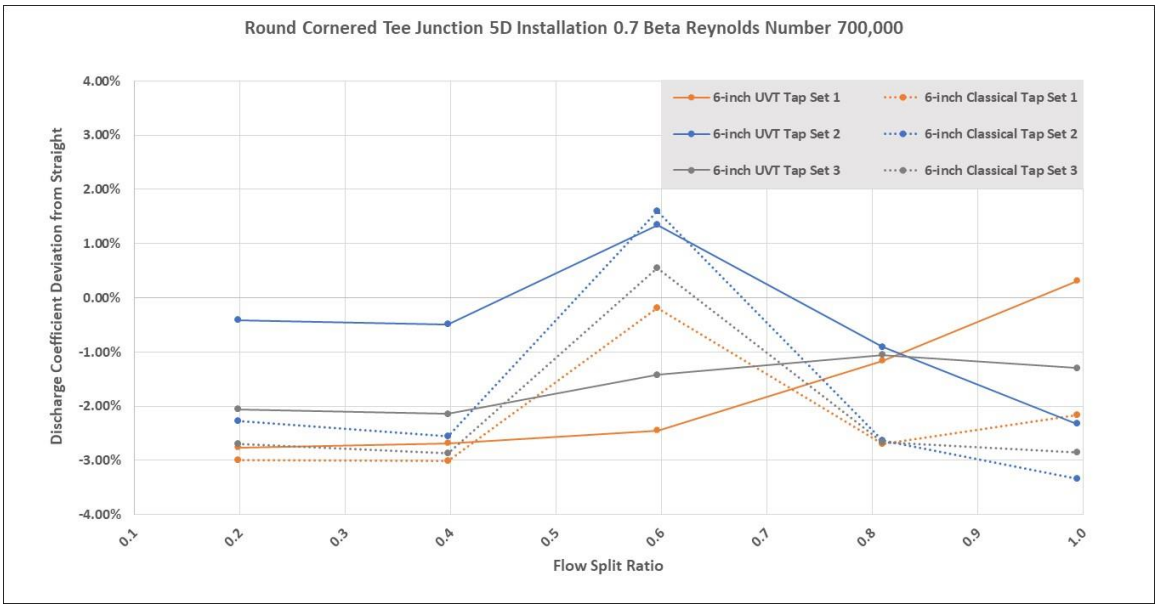

Figure 21. Plot of discharge coefficient deviation from straight versus flow split for a 6-inch UVT and 6-inch Classical Venturi both with 0.7 beta installed 5D from a round cornered tee junction.

Meter Beta Value

For this analysis two 6-inch UVT meters are modeled at 5D, one with a beta value of 0.7 and the other having a beta value of 0.5 with Reynolds Number 700,000 in the pipe entering the tee junction. These are typical high and low beta values for Classical Venturi flowmeters. Figure 15 demonstrates that as the beta value of the meter decreases, or in other words the diameter of the throat relative to the inlet gets smaller, meter accuracy increases over the entire range of flow splits for every tap set. Tap Set 1 shows 60% improvement in accuracy for flow splits between 20% and 60%, a 50% improvement for the 80% flow split, and an 80% improvement when all flow is directed through the meter. Tap Set 2 has varying magnitudes of improvement over the entire flow range, but most

notably, the peak at 60% flow split is improved by 65%. Tap Set 3 on average has 65% greater accuracy with a beta value of 0.5 than with a beta value of 0.7.

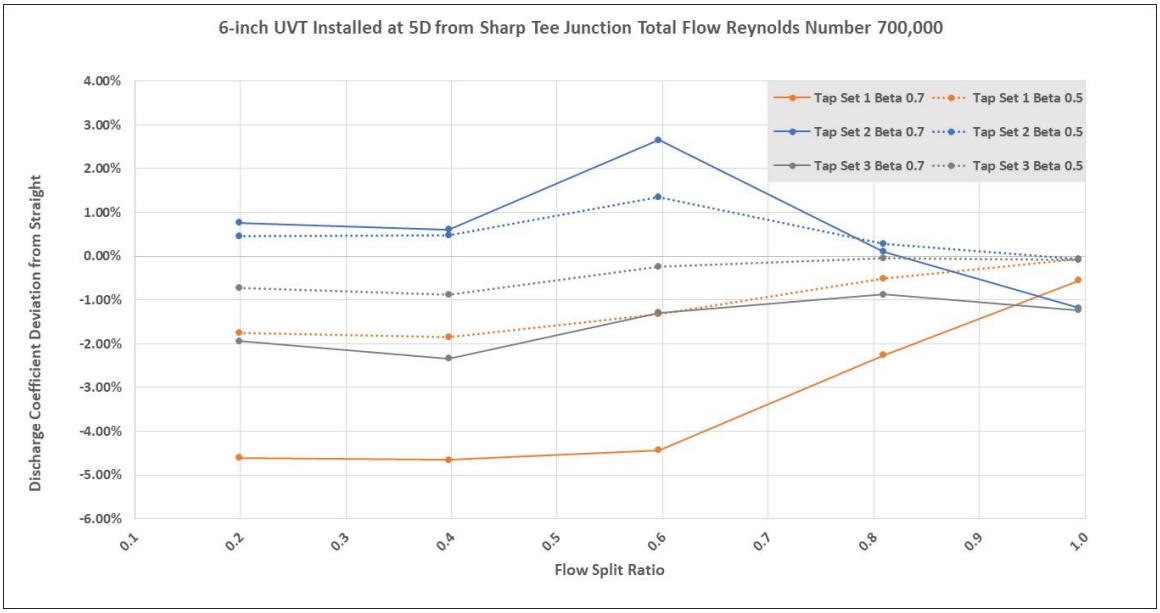

Figure 22. Plot of discharge coefficient deviation from straight versus flow split for two 6-inch UVT meters one with 0.7 beta and the other with 0.5 beta installed 5D from a sharp cornered tee junction.

It is important to consider for this analysis that at 5D all data points still land between +2.8% and -4.8% of the straight-line calibration. The trends from the 0.7 beta and 0.5 beta do not change much, however, the increase in accuracy for every tap over the entire flow range proves that a meter's beta value is a critical factor for metering accuracy when installed downstream of a tee junction on the through leg.

With an understanding about how each of these variables discussed in this chapter affect metering accuracy, it is clear where to focus when performing CFD simulations. The author ran additional simulations to provide the reader with 16 contour plots of correction factors for discharge coefficients found in Appendix A. The provided contour

plots were created from simulations using 0D and 5D installations from a round cornered tee junction for a 6-inch UVT meter, and 0D and 5D installation from a sharp cornered tee junction for a 24-inch Classical Venturi meter both with a beta value of 0.7.

Engineering Judgements

One major aspect of performing research is conducting a deep analysis of the data and understanding the limitations of the tools used. This section is intended to help those reading this paper know under what circumstances that these results are valid, what parts of the results may need additional clarification or research, or even when the results should not even be considered.

The first engineering judgement to be made for this research is the software's capability of modeling reality. In the results it was concluded that CFD is a valid tool to predict the trends of flow metering as certain variables are altered. This means that not every data point collected with CFD absolutely represents reality, rather it is predicting a trend. With the physical models used in CFD for this research, the accuracy of CFD as a predictive tool decreases when there is turbulence or swirling in the flow within the metering range of the flow volume. This is particularly true for the 0D installations with flow splits of 40% or less where flow swirls occur around the high tap of Tap Set 2 as seen in figure 16.

With this in mind, when modeling difficult flow regimes as these, it is important to choose physical models that better account for turbulence and flow swirls. However, in real world applications looking at a different Tap Set location may be what is needed to get the desired metering accuracy.

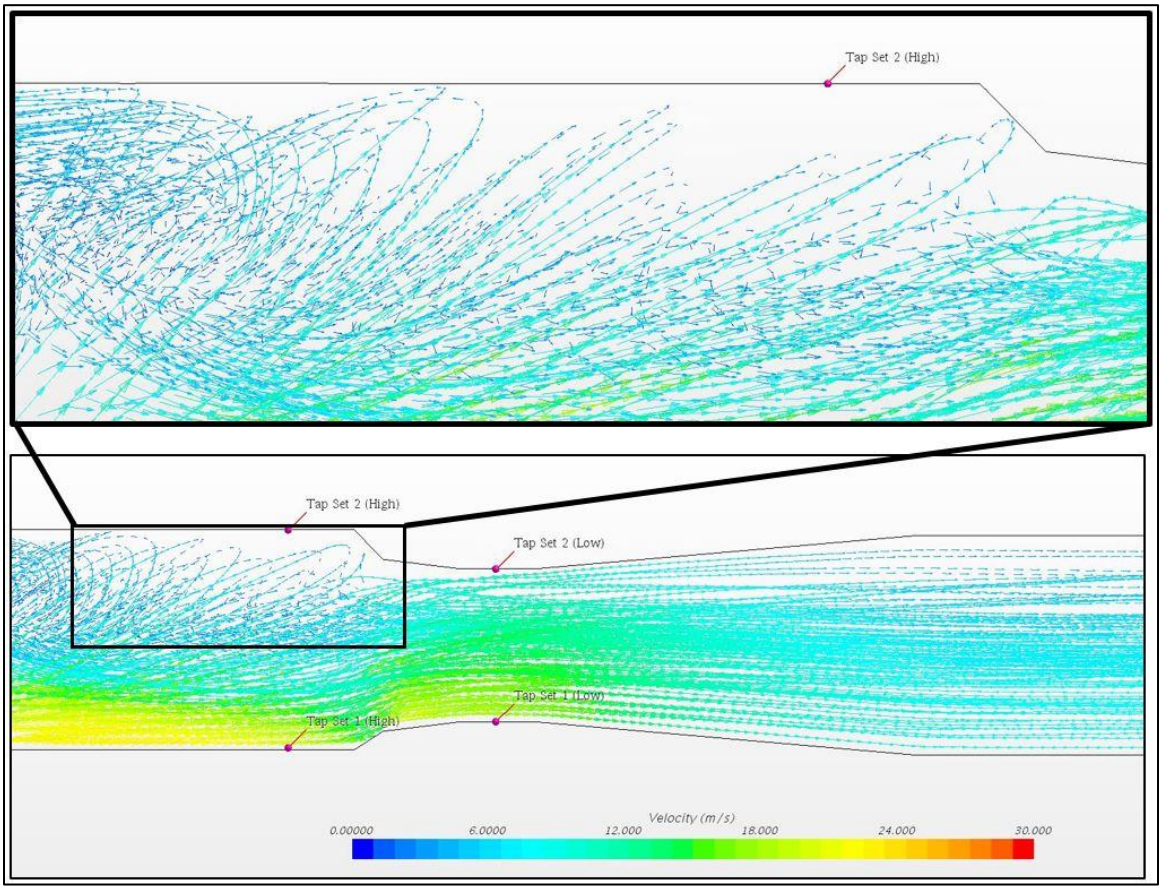

Figure 23. Vector scene of CFD model with 0D installation and 20% flow split.

Looking back at Figure 17 provides several insights into how the data needs to be approached. Starting with Tap Set 1 it is clear to see that the CFD does in fact predict close to the exact percent deviation from the straight line test for flow splits 60% and greater. Below this point at 40% and 20% flow splits however, when using just the CFD data as to calculate correction factors, the flow rate would be over corrected and read about 3 – 3.5% lower than the actual flow rate and the discharge coefficient from the straight-line calibration would perform better over this range of flow splits.

Now examining Tap Set 2, one sees that the CFD data doesn't exactly match the physical data over the entire range of flow splits, in fact it is shifted down about 1 – 1.5%. In this case, if CFD was the only way to calculate correction factors, it wouldn't perform as well as laboratory calibrations of the tee junction installation, but it would perform better than just using the discharge coefficient from the straight-line calibration.

Lastly, the data in figure 17 presents a very intriguing aspect. The physical data for Tap Set 3 hardly shifts from the straight-line calibration at all over the entire range of flow splits. Additionally, the CFD data is shifted down anywhere from 1-2%. This indicates that using CFD to calculate correction coefficients in this case would produce flow rates 1-2% lower than the actual flow rate, where if the discharge coefficient from the straight-line calibration were used, the flow would read accurately to within 0.15% over the entire range of flow splits.

Similar judgement calls need to be made about every set of data collected for this research and any data produced by someone venturing to reproduce or use a similar procedure to correct flow rate measurement on a Classical Venturi flowmeter.

Example for Using Contour Plots

Once all the data has been collected and the contour plots created, knowing how to properly use implement it is crucial. This section provides a detailed example on how to use the contour plots generated with the CFD simulations to adjust the flow equation for a physical meter installed downstream of a tee junction on the through leg.

This example shows this process by using the physical and CFD data collected on the 6-inch UVT meter with 0.7 beta ratio on Tap Set 1 installed 0D. The data point

selected to analyze for this example was at a total flow rate of 1745.0 gpm and a differential pressure across the UVT of 0.261 psi. From the data collected, it is known that 349 gpm is flowing through the UVT. The meter has a straight-line calibration Cd of 0.981 provided by the manufacturer. This means that under these conditions, the indicated flow would be calculated as follows.

First convert the differential pressure from units of pound per square inch to pounds per square foot.

$$0.261\frac{lb}{\cancel{in^2}} * 144\frac{\cancel{in^2}}{ft^2} = 37.584\frac{lb}{ft}$$

Now calculate the flow rate in gallons per minute.

$$Q = C_d * A_t * \sqrt{\frac{2 * \Delta P * g_c}{\rho(1-(\beta)^4)}}$$

$$Q = 448.831\frac{gpm}{cfs} * 0.981 * 0.0983\, ft^2 * \sqrt{\frac{2 * 37.584\frac{\cancel{lb}}{\cancel{ft^2}} * 32.17405\frac{\cancel{ft}}{s^2}}{62.4034\frac{\cancel{lb}}{\cancel{ft^3}}\, ft^2 * (1-(0.6962)^4)}}$$

Consolidate the units.

$$Q = 448.831\frac{gpm}{cfs} * 0.981 * 0.0983\, ft^2 * \sqrt{50.66\,\frac{ft^2}{s^2}}$$

$$Q = 448.831\frac{gpm}{\cancel{cfs}} * 0.981 * 0.0983\cancel{ft^2} * 7.12\,\frac{\cancel{ft}}{\cancel{s}}$$

$$Q = 308.05\, gpm$$

The meter indicates that the flow is 308.05 gpm which is 11.73% lower than the actual flow rate. To start the flow rate adjustment process, the meter Reynolds number and the flow split must be calculated as follows.

$$Reynolds = \left(\frac{\frac{308.05\ \cancel{gpm}}{448.831 \frac{\cancel{gpm}}{\frac{\cancel{ft^3}}{\cancel{sec}}}}}{0.25 * \pi * \left(\frac{6.097\ \cancel{in}}{12 \frac{\cancel{in}}{\cancel{ft}}} \right)^2} \right) * \frac{\left(\frac{6.097 \cancel{in}}{12 \frac{\cancel{in}}{\cancel{ft}}} \right)}{.0000137 \frac{\cancel{ft^2}}{\cancel{sec}}} \approx 125543.1$$

$$Split = \frac{308.05}{1745.0} = 0.177$$

Once these values are obtained, the Cd adjustment value can be extracted from the contour plot as seen in Figure 16. In this case, a flow split of 0.2 will be used because there is no data below this point.

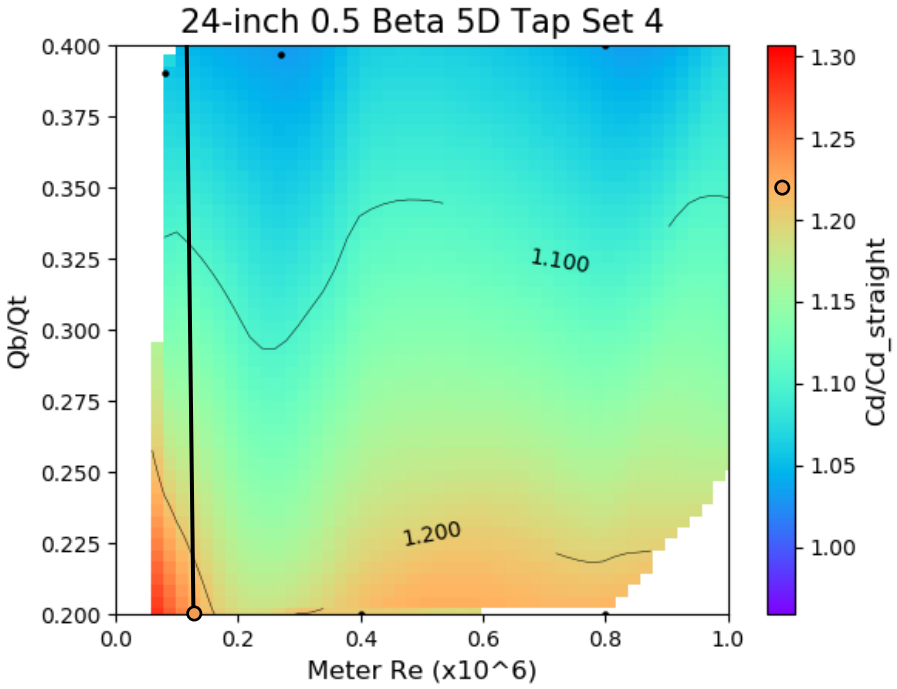

Figure 24. Contour plot for Tap Set 1 of the CFD 6-inch UVT 0.7 beta 0D installation.

From Figure 16 the adjustment factor 1.23 is extracted and used in the following calculation to find a new indicated flow rate.

$$Q_{adjusted} = \frac{C_d}{C_{d\ strait}} * C_d * A_t * \sqrt{\frac{2 * \Delta P * g_c}{\rho(1-(\beta)^4)}}$$

$$Q\ = 1.23 * 448.831 \frac{gpm}{cfs} *\ 0.981 * 0.0983\ ft^2 * \sqrt{\frac{2 * 37.584 \frac{\cancel{lb}}{\cancel{ft^2}} * 32.17405 \frac{\cancel{ft}}{s^2}}{62.4034 \frac{\cancel{lb}}{\cancel{ft^3}\ ft^2} * (1-(0.6962)^4\ )}}$$

$$Q\ = 378.9\ gpm$$

After one iteration of this process, the meter shows an adjusted flow rate of 378.9 gpm which is 8.56% higher than the actual flow going through the meter. This process is meant to be iterated until the change in adjusted flow rate from one iteration to the next does not change. To fulfill the purpose of this example one more iteration will be needed. Start the next iteration by calculating the new Meter Reynolds number.

$$Reynolds = \left(\frac{\frac{378.9\ \cancel{gpm}}{448.831 \frac{\cancel{gpm}}{\frac{\cancel{ft^3}}{\cancel{sec}}}}}{0.25 * \pi * \left(\frac{6.097\ \cancel{in}}{12 \frac{\cancel{in}}{\cancel{ft}}} \right)^2} \right) * \frac{\left(\frac{6.097 \cancel{in}}{12 \frac{\cancel{in}}{\cancel{ft}}} \right)}{.0000137 \frac{\cancel{ft^2}}{\cancel{sec}}} \approx 154417.4$$

$$Split = \frac{378.9}{1745.0} = 0.217$$

Once these values are obtained, the Cd adjustment value can be extracted from the contour plot as seen in Figure 16.

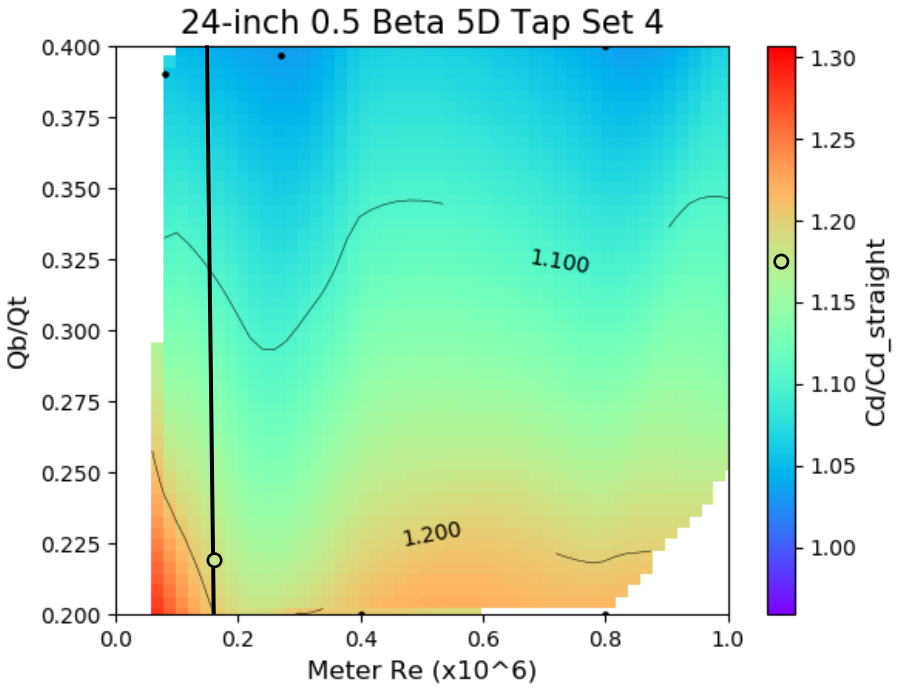

Figure 25. Contour plot for Tap Set 1 of the CFD 6-inch UVT 0.7 beta 0D installation.

From Figure 16 the adjustment factor 1.175 is extracted and used in the following calculation to find a new indicated flow rate.

$$Q_{adjusted} = \frac{C_d}{C_{d\ strait}} * C_d * A_t * \sqrt{\frac{2 * \Delta P * g_c}{\rho(1-(\beta)^4)}}$$

$$Q\ = 1.175 * 448.831 \frac{gpm}{cfs} *\ 0.981 * 0.0983\ ft^2 * \sqrt{\frac{2 * 37.584 \frac{\cancel{lb}}{\cancel{ft^2}} * 32.17405 \frac{\cancel{ft}}{s^2}}{62.4034 \frac{\cancel{lb}}{\cancel{ft^3}\ ft^2} * (1-(0.6962)^4\ )}}$$

$$Q\ = 361.96\ gpm$$

After the second iteration of this process, the meter shows an adjusted flow rate of 361.96 gpm which is 3.7% higher than the actual flow going through the meter. This example shows that within two iterations of applying correction factors, there is a 68.3% improvement in flow rate accuracy.

CHAPTER V

CONCLUSION

Differential pressure producing flowmeters are used in many industrial and municipal applications. Ensuring that these meters accurately measure flow rate is of high importance in these instances to provide processes and consumers with high quality products and services. There is so much importance placed on accurate flow measurement that standards of installation and use have been created to guide proper hydraulic design both upstream and downstream of the meter. However, meeting these standards is not always practical due to space or fiscal constraints.

When pipe systems are designed that place flowmeters in installation contrary to those established by industry or manufacturer standards the best solution is to perform a laboratory calibration of the meter with the same installation specifications as the design. Laboratory calibrations, like those performed at the Utah Water Research Laboratory, are typically cost effective and timely. However, when setup for a calibration requires large sizes needing extra space, manpower, and run time, these calibrations can become expensive. In these cases performing CFD models, although not as accurate as a laboratory calibrations, may be sufficiently accurate.

This research develops a process which readers may use as a template to simulate reasonably similar flowmeters and installation setups. For the case studied in this research, a flowmeter installed downstream of a tee junction on the through leg, three variables, pipe size, tee junction geometry, and the main Reynolds Number entering the tee junction, were all found to have little to no impact on the results.

On the other hand, there are three variables that require more attention in order to get accurate results from the simulations. First, the meter geometry, including the length of the inlet section, angles of contraction and expansion, and the length of the throat must be modeled as close to the physical dimensions possible. Second, the flow splits that are going to be ran through the tee junction in the field must match those flow splits in the simulations. If this cannot be achieved it is important to run enough flow splits to understand the trend of data over the range of flow splits needed. Lastly, modeling the meter beta ratio as close to the physical dimensions is important to understand how that particular meter will perform. Once the volume is meshed, the diameter of the inlet and throat will not be exactly as drawn in the geometry. Adjustments may need to be made to the throat diameter after the first mesh is created.

Once simulations are completed, the data is used to create a contour plot of correctional discharge coefficients that can be used to accurately adjust the flow measurement on the meter. Applying the contour plot to real life systems could then be digitized to reflect real-time accurate readings on the meter.

It is important to note that this research has limitations and proper engineering judgement must be used when applying the findings. These limitations include the modeling capabilities of the software used for simulations, the scope of work only includes an analysis of two meter types, two beta values, and incompressible fluid flow.

Further research is needed to more fully understand the complexities of installing a differential pressure producing flowmeter downstream of a tee junction on the through leg. There are many more types of meters, including wedge meters and Venturi tubes to

list a few, that could be studied. Further research could explore how compressible fluids or even the viscosity of an incompressible fluid changes the results. Additional work could also be done to look at how cavitation above a certain flow rate affects the results. This research topic is far from being completely covered.

REFERENCES

The American Society of Mechanical Engineers (ASME). (2005). “Flow Measurement: An American National Standard.” New York. ASME PTC 19.5-2005.

The American Society of Mechanical Engineers (ASME), 2006. “Test Uncertainty: An American National Standard.” New York. ASME PTC 19.1-2006.

The American Society of Mechanical Engineers (ASME). (2007). “Measurement of Fluid Flow in Pipes Using Orifice, Nozzle and Venturi: An American National Standard.” New York. ASME MFC-3Ma-2007.

Bradford, Jason E., Michael C. Johnson, and J. Gary Gilbert. 2006. “Performance of Venturi Meters Installed Downstream of Bends.” *Journal - American Water Works Association* 98 (4): 156–164.

Day, Matthew P., Michael C. Johnson, and Steven L. Barfuss. 2019. “Flowmeter Performance Comparison Downstream of Double 90° Elbows out-of-Plane.” *AWWA Water Science* 1 (1).

Finnemore, E. J., and Franzini, J. B. (2002). “Venturi meter.” Fluid mechanics with engineering applications, McGraw-Hill, USA, 515–518.Miller, R. W. (1996). *Flow measurement engineering handbook*. New York: McGraw-Hill.

The International Organization of Standardization (ISO). 2003. “Measurement of fluid flow by means of pressure differential devices inserted in circular cross-section conduits running full – Part 4: Venturi tubes.” Geneva. ISO 5167-4:2003.

Pereira, M. D. “Flow Meters: Part 1 Part 18 in a series of tutorials in instrumentation and measurement.” *IEEE Instrumentation & Measurement Magazine* 12 (2009): 18-26.

Radle, D. (2016). *Effects on a wedge flowmeter installed downstream of a double elbow out of plane.* (Master's thesis). School of Mechanical Engineering, Utah State University, Logan, Utah.

Sandberg, Benjamin G., "Venturi Flowmeter Performance Installed Downstream of the Branch of a Tee Junction" (2020). *All Graduate Theses and Dissertations*. 7825. https://digitalcommons.usu.edu/etd/7825

Siemens. (2020). “Reynolds-Averaged Navier-Stokes (RANS) Turbulence Models.” <https://documentation.tehsteveportal.plm.automation.siemens.com/starccmplus_latest_en/index.html#page/STARCCMP%2FGUID-7237C585-2707-4FCC-BB3F-E2376C68B114.html> (Feb. 28, 2020).

Singh, Rajesh Kumar, S.n. Singh, and V. Seshadri. 2010. “CFD Prediction of the Effects of the Upstream Elbow Fittings on the Performance of Cone Flowmeters.” *Flow Measurement and Instrumentation* 21 (2): 88–97.

Stauffer, Taylor B., Michael C. Johnson, Zachary B. Sharp, and Steven L. Barfuss. 2019. “Multiple Tap Sets to Improve Venturi Flowmeters Performance Characteristics with Disturbed Flow.” *AWWA Water Science* 1 (3).

APPENDICES

APPEDENDIX A

CONTOUR PLOTS

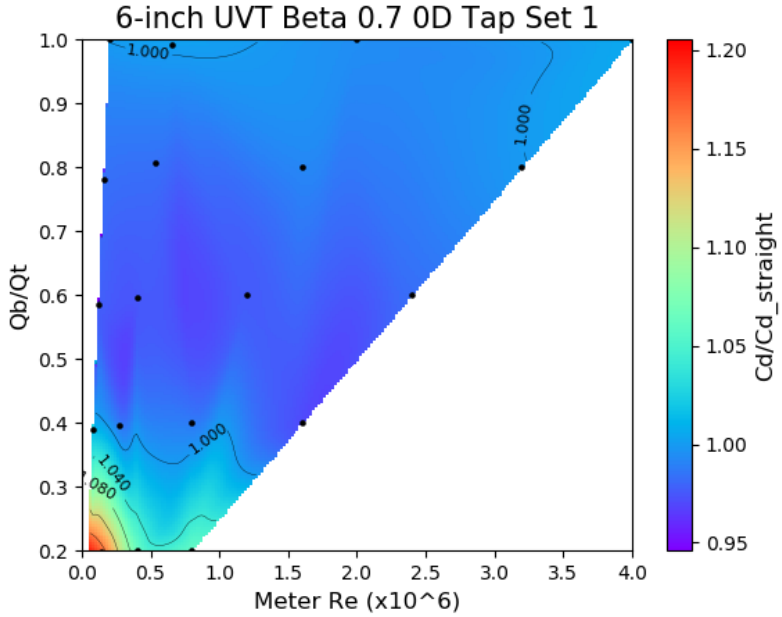

Figure A1. Contour plot for Tap Set 1 of the CFD 6-inch UVT 0.7 beta 0D installation.

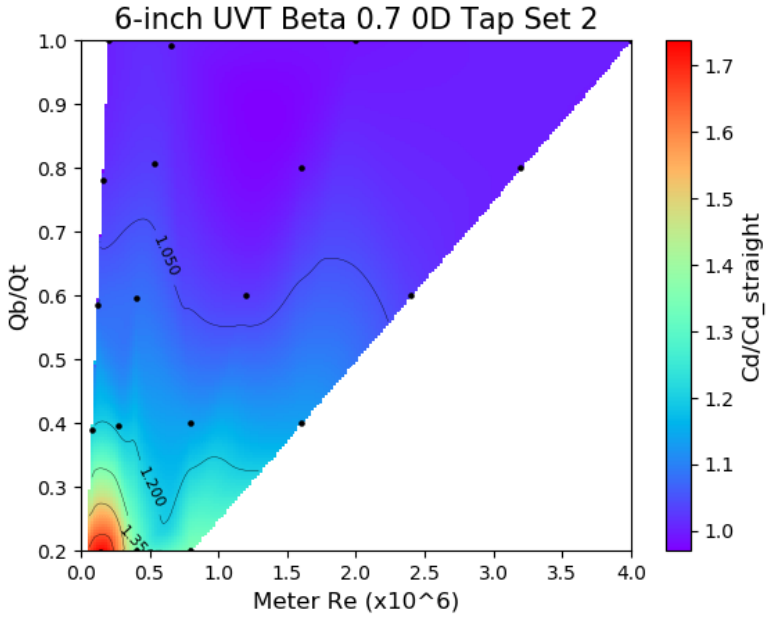

Figure A2. Contour plot for Tap Set 2 of the CFD 6-inch UVT 0.7 beta 0D installation.

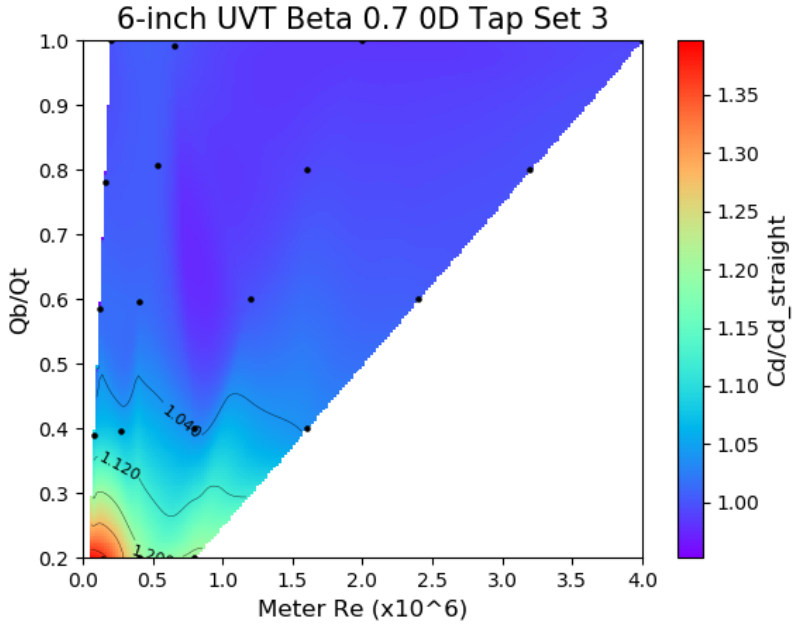

Figure A3. Contour plot for Tap Set 3 of the CFD 6-inch UVT 0.7 beta 0D installation.

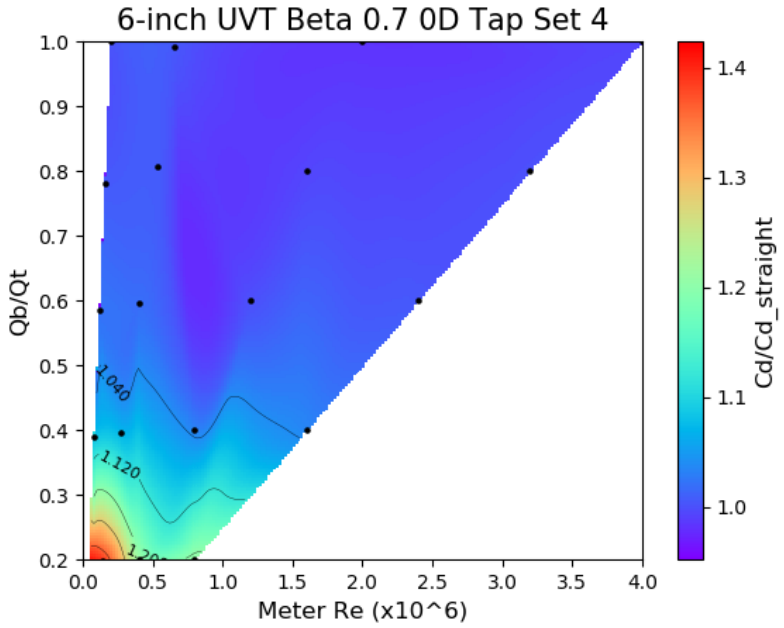

Figure A4. Contour plot for Tap Set 4 of the CFD 6-inch UVT 0.7 beta 0D installation.

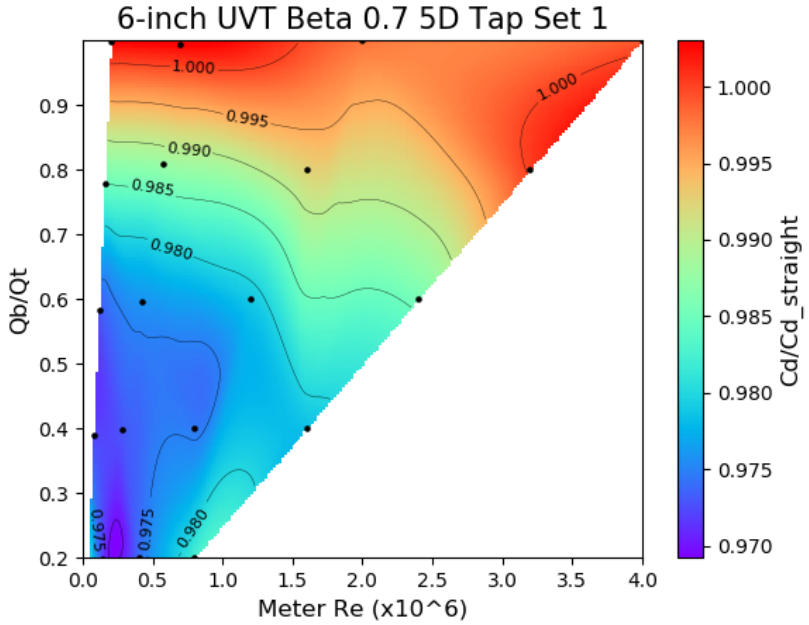

Figure A5. Contour plot for Tap Set 1 of the CFD 6-inch UVT 0.7 beta 5D installation.

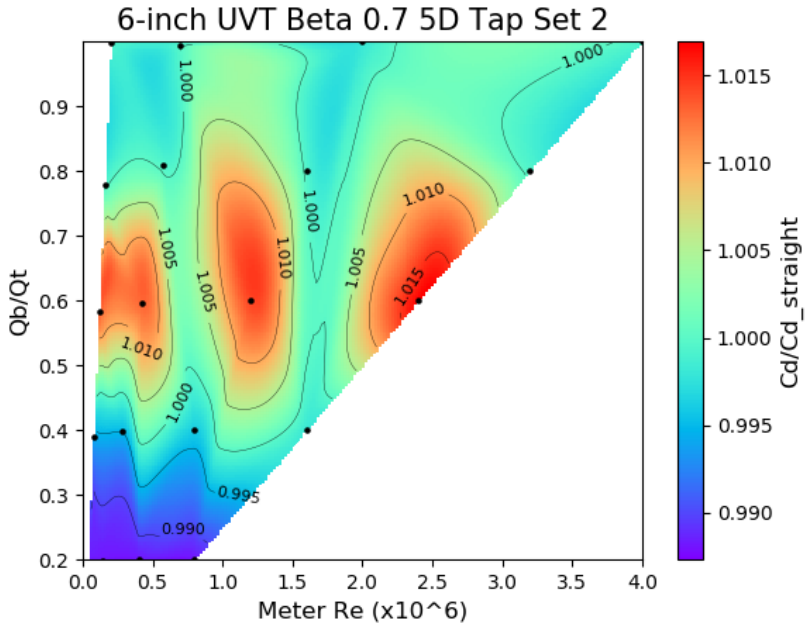

Figure A6. Contour plot for Tap Set 2 of the CFD 6-inch UVT 0.7 beta 5D installation.

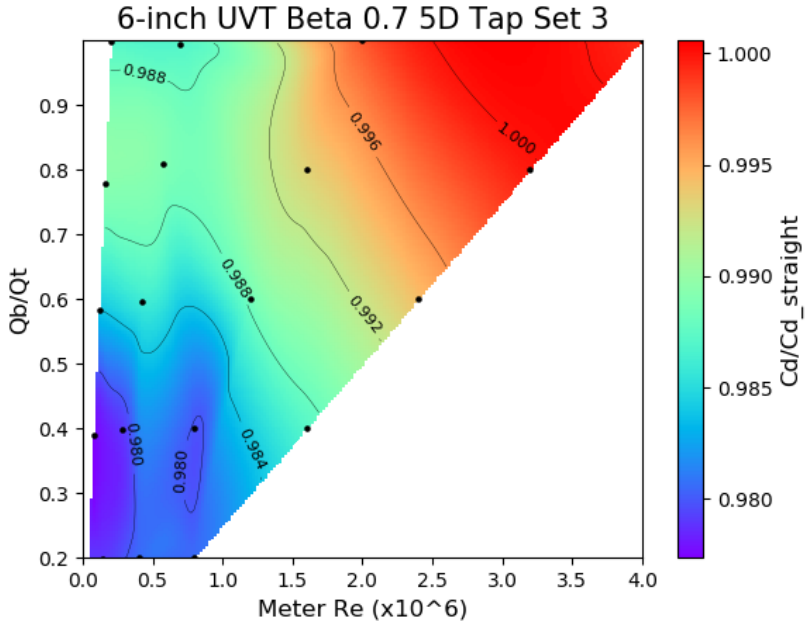

Figure A7. Contour plot for Tap Set 2 of the CFD 6-inch UVT 0.7 beta 5D installation.

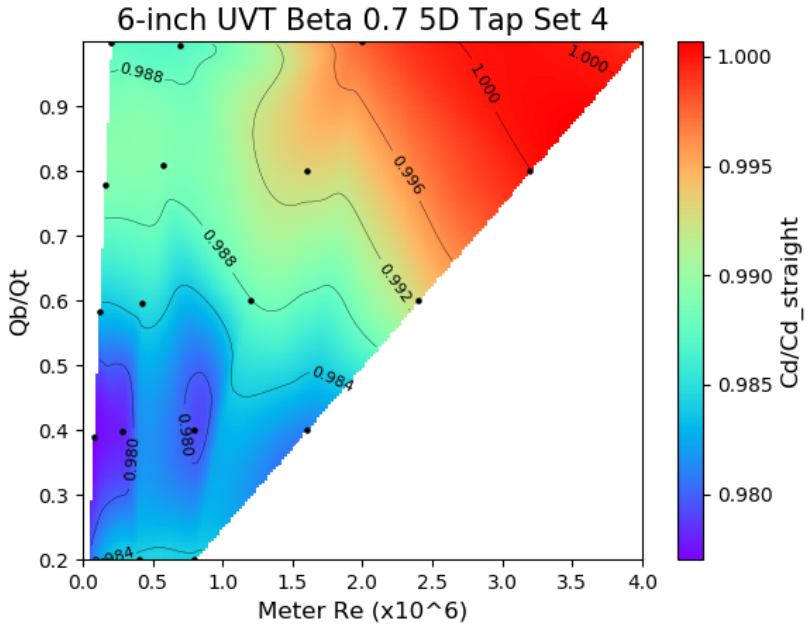

Figure A8. Contour plot for Tap Set 3 of the CFD 6-inch UVT 0.7 beta 5D installation.

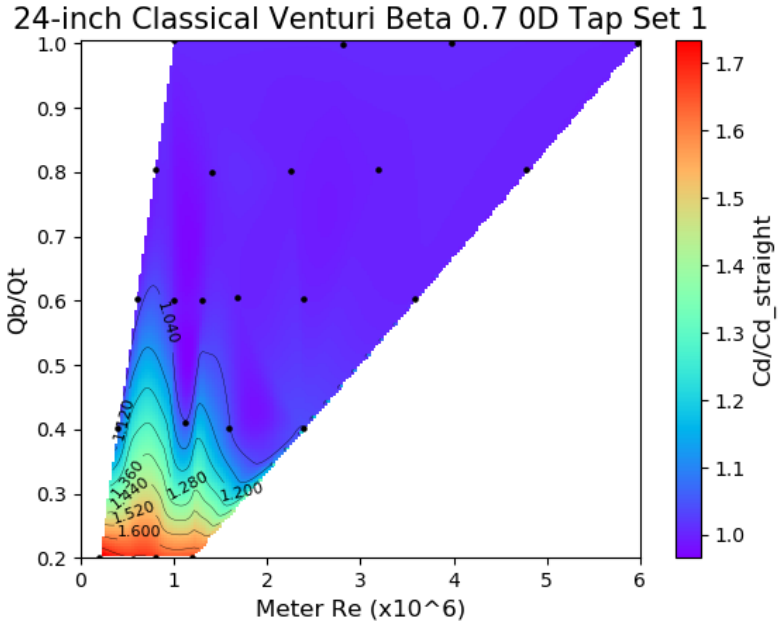

Figure A9. Contour plot for Tap Set 1 of the CFD 24-inch Classical 0.7 beta 0D installation.

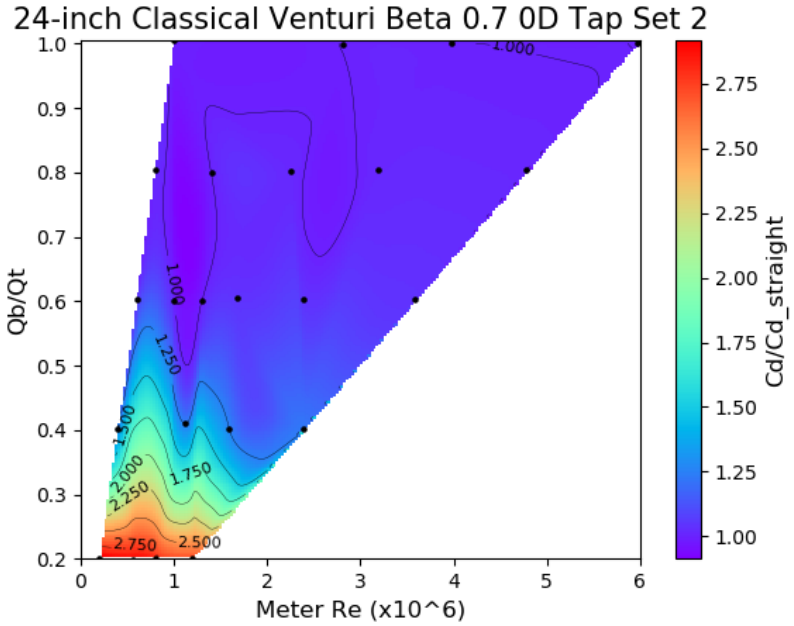

Figure A10. Contour plot for Tap Set 2 of the CFD 24-inch Classical 0.7 beta 0D installation.

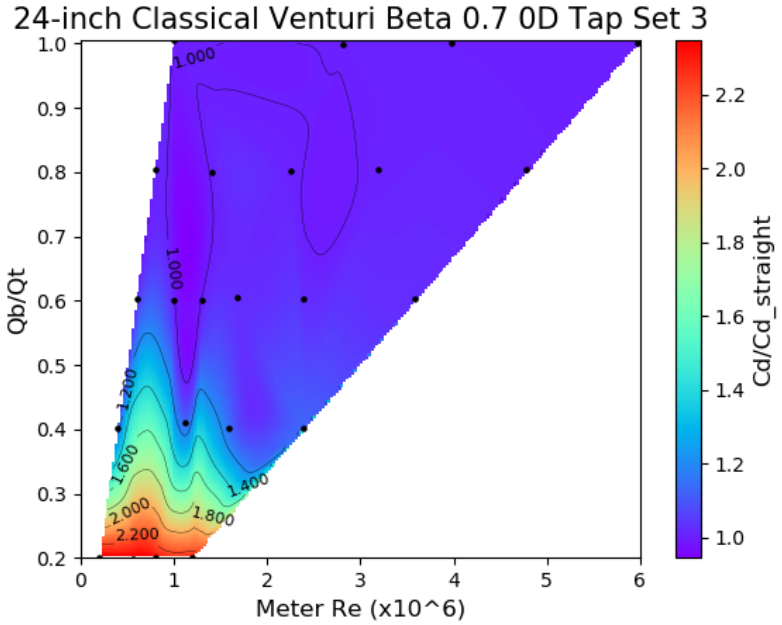

Figure A11. Contour plot for Tap Set 3 of the CFD 24-inch Classical 0.7 beta 0D installation.

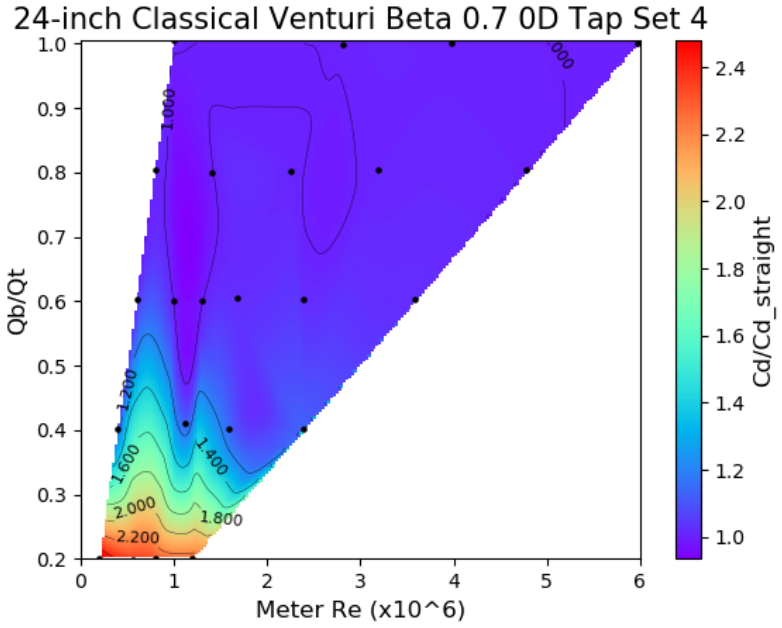

Figure A12. Contour plot for Tap Set 4 of the CFD 24-inch Classical 0.7 beta 0D installation.

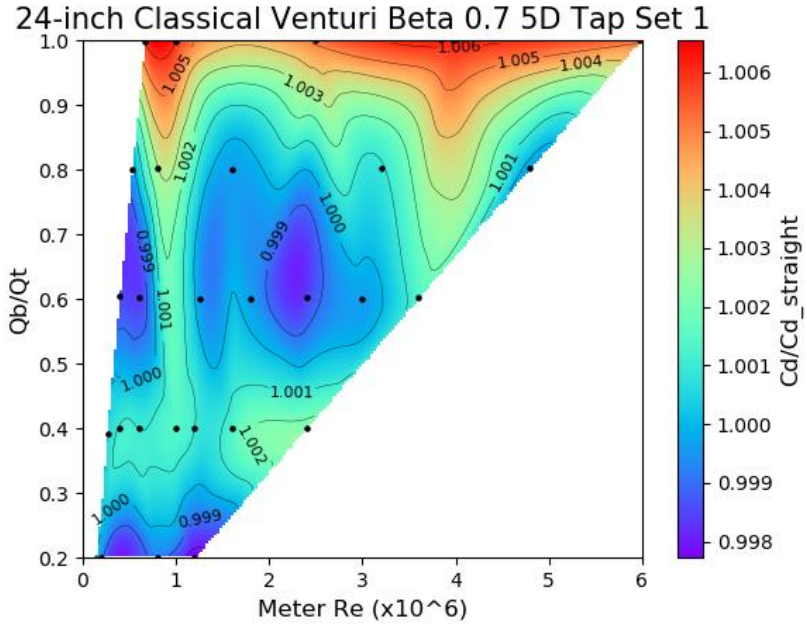

Figure A13. Contour plot for Tap Set 1 of the CFD 24-inch Classical 0.7 beta 5D installation.

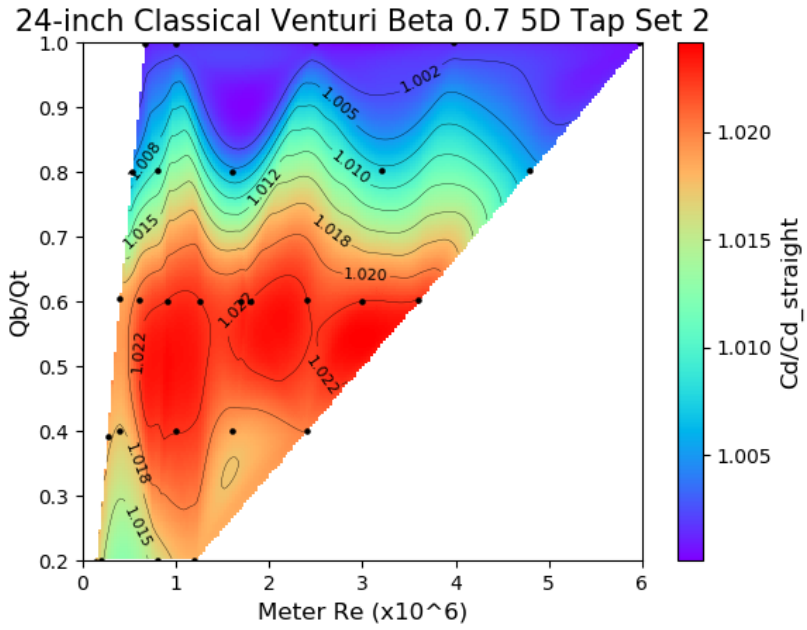

Figure A14. Contour plot for Tap Set 2 of the CFD 24-inch Classical 0.7 beta 5D installation.

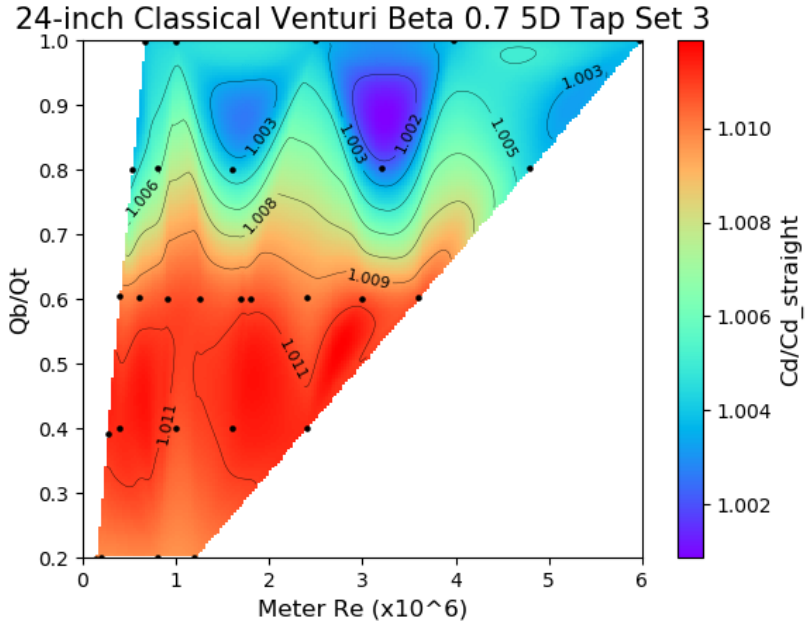

Figure A15. Contour plot for Tap Set 3 of the CFD 24-inch Classical 0.7 beta 5D installation.

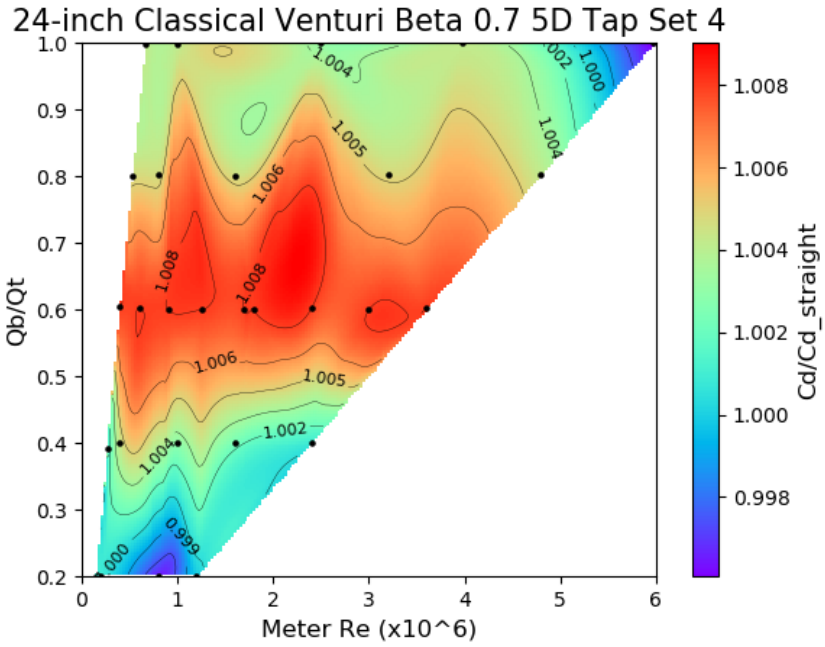

Figure A16. Contour plot for Tap Set 4 of the CFD 24-inch Classical 0.7 beta 5D installation.

APPENDIX B

ADDITIONAL GRAPHS AND DIMENSIONAL DRAWINGS

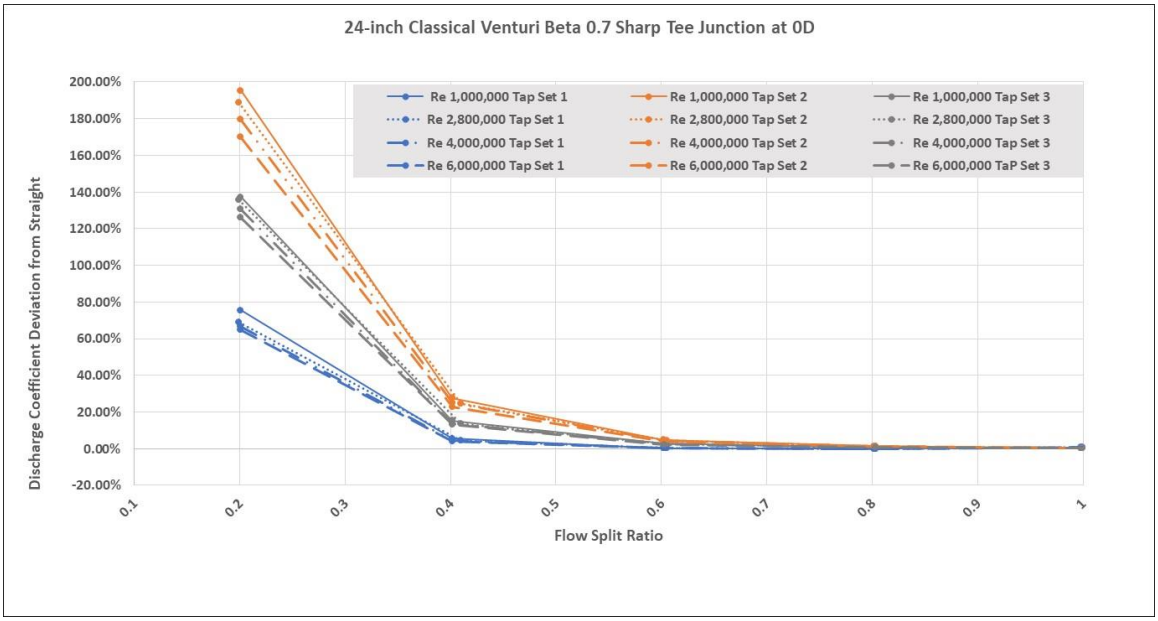

Figure B1. Plot of discharge coefficient deviation from straight versus flow split for a 24-inch Classical Venturi with 0.7 beta installed 0D from a sharp tee junction.

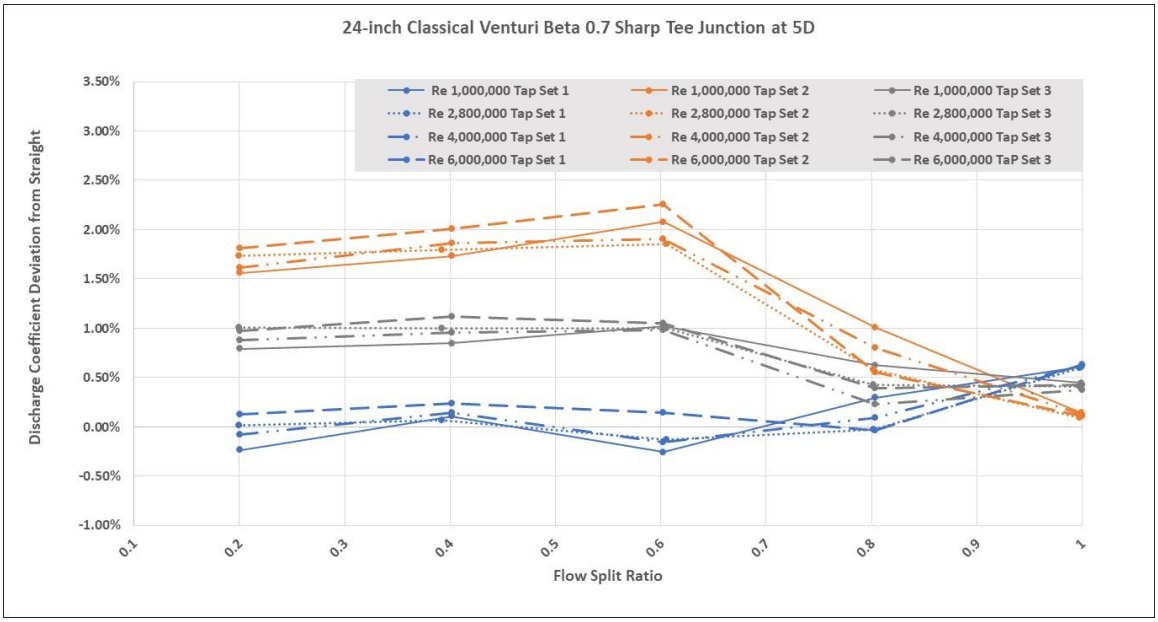

Figure B2. Plot of discharge coefficient deviation from straight versus flow split for a 24-inch Classical Venturi with 0.7 beta installed 5D from a sharp tee junction.